TIARA-NOTE-WP9-2014-001

Test Infrastructure and Accelerator Research Area

Scientific / Technical Note

Detail Engineering Design T-MIF

Fusco, Y. (CERN)

12 February 2014

The research leading to these results has received funding from the European Commission under the FP7-INFRASTRUCTURES-2010-1/INFRA-2010-2.2.11 project TIARA (CNI-PP). Grant agreement no 261905.

This work is part of TIARA Work Package **9: TIHPAC R&D Infrastructure**.

The electronic version of this TIARA Publication is available via the *TIARA web site* at `http://www.eu-tiara.eu/database` or on the *CERN Document Server* at the following URL: `http://cds.cern.ch/search?p=TIARA-NOTE-WP9-2014-001`

Test Infrastructure and Accelerator Research Area

Technical Note

Detail Engineering Design
T-MIF

Fusco, Y. (CERN)

22. January 2014

The research leading to these results has received funding from the European Commission under the FP7-INFRASTRUCTURES-2010-1/INFRA-2010-2.2.11 project TIARA (CNI-PP).
Grant agreement no 261905.

This work is part of TIARA Work Package 9: TIHPAC R&D Infrastructure.

TIARA Project

Work Package 9: TIHPAC - Test Infrastructure for High Power Accelerator Components

Task 9.1: Multi MW Irradiation Facility for complex target testing

TN n ° 01: Engineering design and analysis of the Heat Exchanger for T-MIF

Planned Date (month):36

Achieved Date (month):29 **(contribution to final report due month 36)**

Lead Contractor:CERN

Project acronym:	*TIARA*
Project full title:	*Test Infrastructure in Accelerator Research Area*
Start of the Project:	*1st January 2011*
Duration of the project:	*36 Months*
Author:	*Yoann Fusco* *Design engineer*
Lead engineer:	*Karel Samec* *Nucl. Eng., Mech. Eng.*
Task Coordinator:	*Yacine Kadi* *Prof. Dr. Phys.*

Contents

F i g u r e s

T a b l e s

R e f e r e n c e s

Ref. 1: K. Samec: "Report on the Definition and Specifications of the Irradiation test Facilities", TIARA-REP-WP9-2012-001, FP7-Infrastructures-2010-1/INFRA-2010-2.2.11 project TIARA, 23 January 2012

Ref. 2: K. Samec: "Preliminary design report for a high-power Material Irradiation Facility T-MIF", TIARA-REP-WP9-2013-XXX, FP7-Infrastructures-2010-1/INFRA-2010-2.2.11 project TIARA, 25 February 2013

Ref. 3: Y. Fusco, M. Berzhad: "Thermal-hydraulic analysis of the neutron source for T-MIF", TIARA-REP-WP9-2014-XXX, FP7-Infrastructures-2010-1/INFRA-2010-2.2.11 project TIARA, January 2014

Ref. 4: R. Luis, Y. Romanets : "Neutronics FLUKA analysis of the Target section for T-MIF", TIARA-REP-WP9-2014-XXX, FP7-Infrastructures-2010-1/INFRA-2010-2.2.11 project TIARA, January 2014

Ref. 5: K. Samec "Cost estimate and work package breakdown for T-MIF", TIARA-REP-WP9-2014-XXX, FP7-Infrastructures-2010-1/INFRA-2010-2.2.11 project TIARA, January 2014

S y m b o l s

Parameters, variables and abbreviations:

CERN	Abbr.	Centre Européen de la Recherche Nucléaire, Switzerland
C_P	[J/kg/K]	Thermal capacity
CFD	Abbr.	Computational Fluid Dynamics
dpa	Abbr.	Displacement per atom
FEM	Abbr.	Finite Element Method
f	[Hz]	Frequency
LM	Abbr.	Liquid Metal
T	[°C]	Temperature
t	[sec.]	Time
Δ	[-]	Discrete difference, change
ϕ	[$n/cm^3/s$]	Neutron flux
λ	[W/m/s]	Thermal conductivity
ρ	[kg/m^3]	Density

1 Design of the T-MIF facility

As set out in the specification report (Ref. 1) the design of the T-MIF facility aims at obtaining the greatest possibility flexibility in terms of its use in different beam irradiation facilities around the world, while ensuring safety and minimising down-time for repairs and maintenance.

Research establishments where the test facility would be installed would not necessarily dispose of the full range of nuclear installations such as hot cells that are usually required for maintenance of installations under high irradiation. Therefore a modular solution has been proposed, in which the most activated components can be disassembled and stored for a period of time until the activity has decayed sufficiently that they may be accessed under less stringent requirements. The modular construction also helps in cases of accidents by isolating the most affected equipment which may then be disposed of as a global waste package.

An overall concept for fulfilling these goals has been laid out in the preliminary design report for the entire facility (Ref.2) which gives more detail on the engineering aspects of the various components. After a review of similar installations and in light of past experience, the essential parameters of the facility are chosen as follows:

Power Exchanged	100 kW
Primary side fluid	Lead or LBE or Mercury
Secondary side fluid	Gallium
Specific requirements	Leak-proof Leak detection Able to disconnect primary/secondary Gravity-fed in case of pump trip Smallest inventory primary-side
Pressure	12 Bar

Table 1: Essential thermal hydraulic characteristics of the facility

The primary side fluid was given much thought. The choice of primary liquid depends on the type of application pursued, i.e. material research, radio-pharmaceutical production or rare isotope research. In the present case, both LBE and lead were calculated in subsequent sections in terms of heat exchange and found to be acceptable. Mercury was not calculated but would also be acceptable in that respect since it imposes fewer difficulties, due to its state as a liquid at room temperature.

Analysis proved Gallium to be an adequate choice for evacuating the heat form the primary fluid and passing it on to the cold source, materialised in the facility by an air-cooled heat exchanger.

The components were placed in a manner to optimise space requirements whilst taking into account the necessities of shielding. The process for arriving at an optimal solution in terms of shielding may be found in Ref.4, whilst the process of optimising the target is detailed in reference 3. Hence these aspects will not be addressed in detail in the current document.

The next following pages detail the overall concept, whilst details of specific components that were not covered by dedicated analyses in Ref.3 and 4 are explained in dedicated sections thereafter. The final design shown in the figure hereafter is the result of an optimisation which by virtue of conflicting demands has had to make some compromises, the most challenging of which was to fit the entire facility within a very tight space.

1.1 Overall layout of the primary loop

The primary loop and its component are shown below, separate from the secondary loop and without any shielding for greater clarity. Individual aspects of the different components are explained in greater detail in the following sections. The circulation of the fluid is highlighted by the arrows.

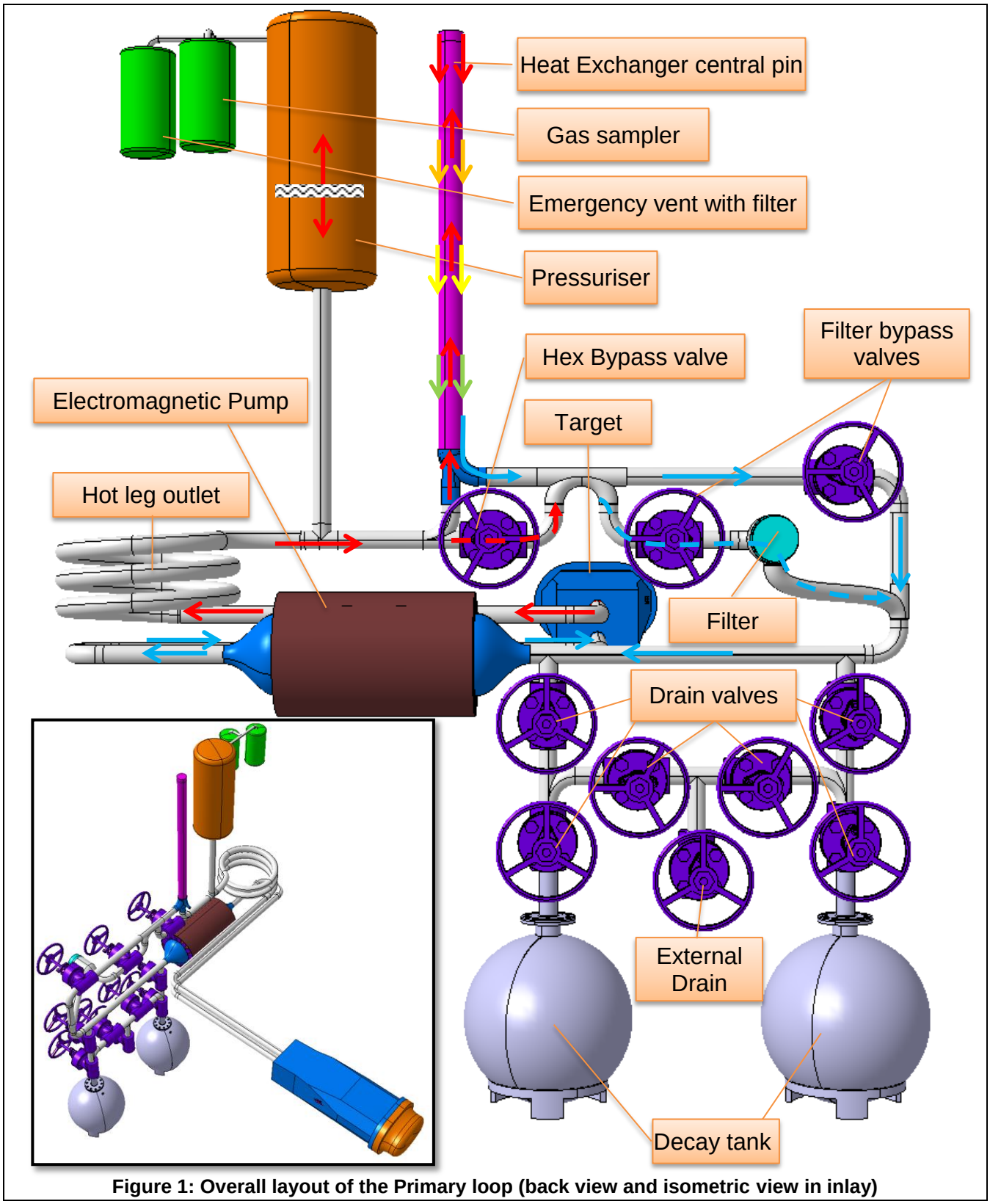

Figure 1: Overall layout of the Primary loop (back view and isometric view in inlay)

As may be seen in the figure above, all the components of the primary loop are organised in such a manner to facilitate operation and maintenance. In particular;

- The pipes lengths are minimized to keep the total volume of activated liquid in the primary circuit low.
- The assembly is as compact as possible to leave more space for the shielding around the target, all which is fitted in a cube, 2 meter on a side.
- The decay sump tanks are at the lowest position to ensure that all the liquid in the primary flows out of the loop by gravity when it is drained.
- The pump is situated in the cold leg just before the target station, to provide maximum protection against thermal transients by using the inertia of the loop.
- The target outlet hot leg features a series of hoops to absorb any thermal expansion due to the temperature variations and to minimise associated stresses in the system.
- The pressuriser tank, gas sampler and emergency venting system are located at the highest point of the primary loop, which is essential for maintaining pressure equilibrium in the loop and ensuring spallation gases are continuously vented form the liquid.
- The heat exchanger is located at the highest position to allow gravity-driven flow to continue cooling the target in the event of a pump failure.
- A heat exchanger by-pass is implemented as a simple means of controlling the temperature in the loop by allowing a variable portion of the hot fluid leaving the target to bypass the heat exchanger. Thus the temperature can be controlled independently of the flow-rate.
- Ease of access to all the components needed for operation such as valves and the filter is ensured by locating them in the same plane at the back of the facility.

This facility is designed to be transportable; the entire components are fixed to a frame in the shape of a 2 metre cube. A sump plate below the frame is foreseen collect any eventual leaks. A system of articulated roller transport trollies or air-pads is designed to allow transport and positioning.

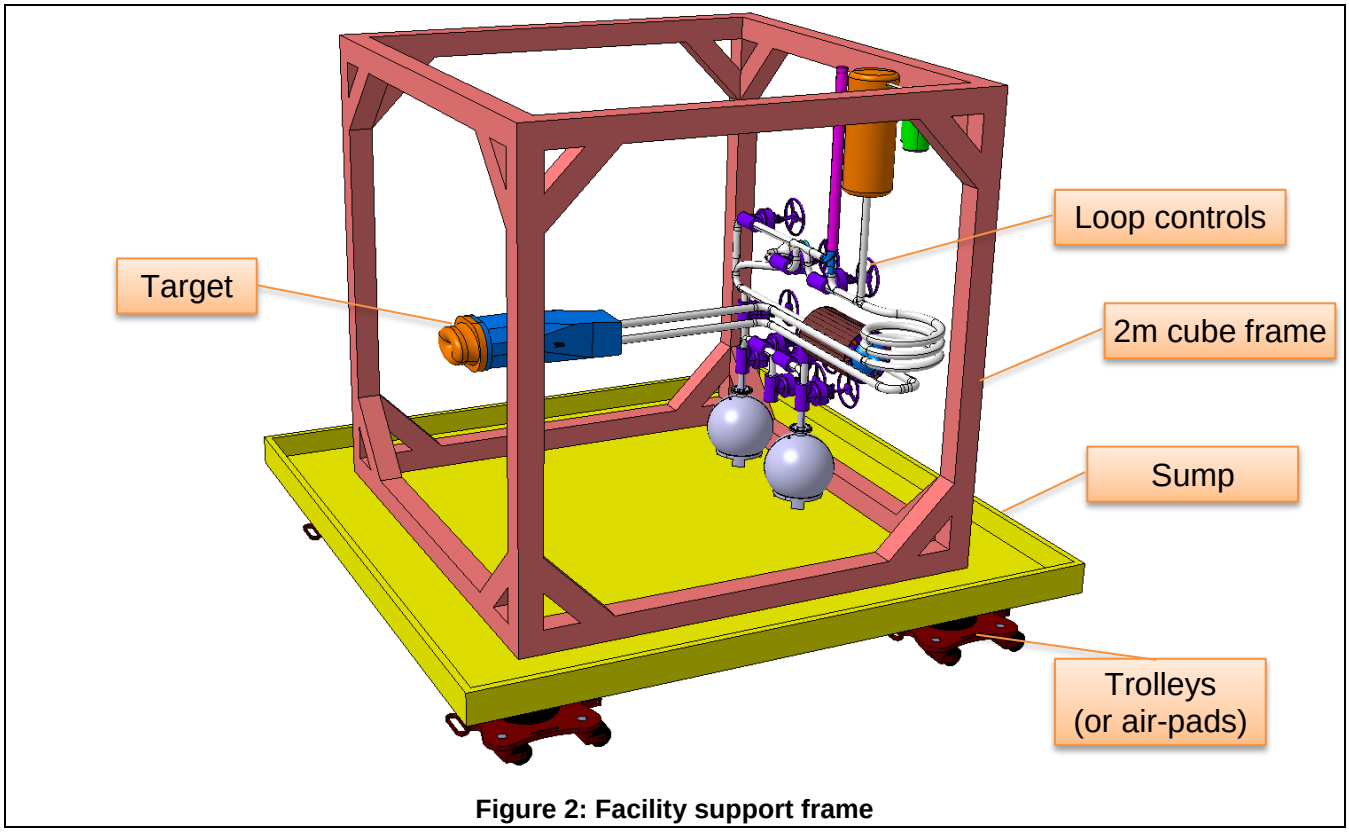

Figure 2: Facility support frame

1.2 Shielding

The shielding encompasses the full dimensions of the frame, absorbing all the components within it. It has been optimised as explained in Ref.4, by dedicated shielding around the target and by heavily shielding the two decay tanks at the bottom of the facility which receive the entire content of the primary loop after shut-down. Indeed, the hydrogen-rich polyethylene serves to moderate the neutrons escaping the central spallation target, while the last layer of borated polyethylene helps in neutron capture and the lead around the target and tanks shields from gammas due to activation. The shielding requires a large volume and thus absorbs many components of the facility in which access holes and recesses have to be designed to allow operation and maintenance of the facility.

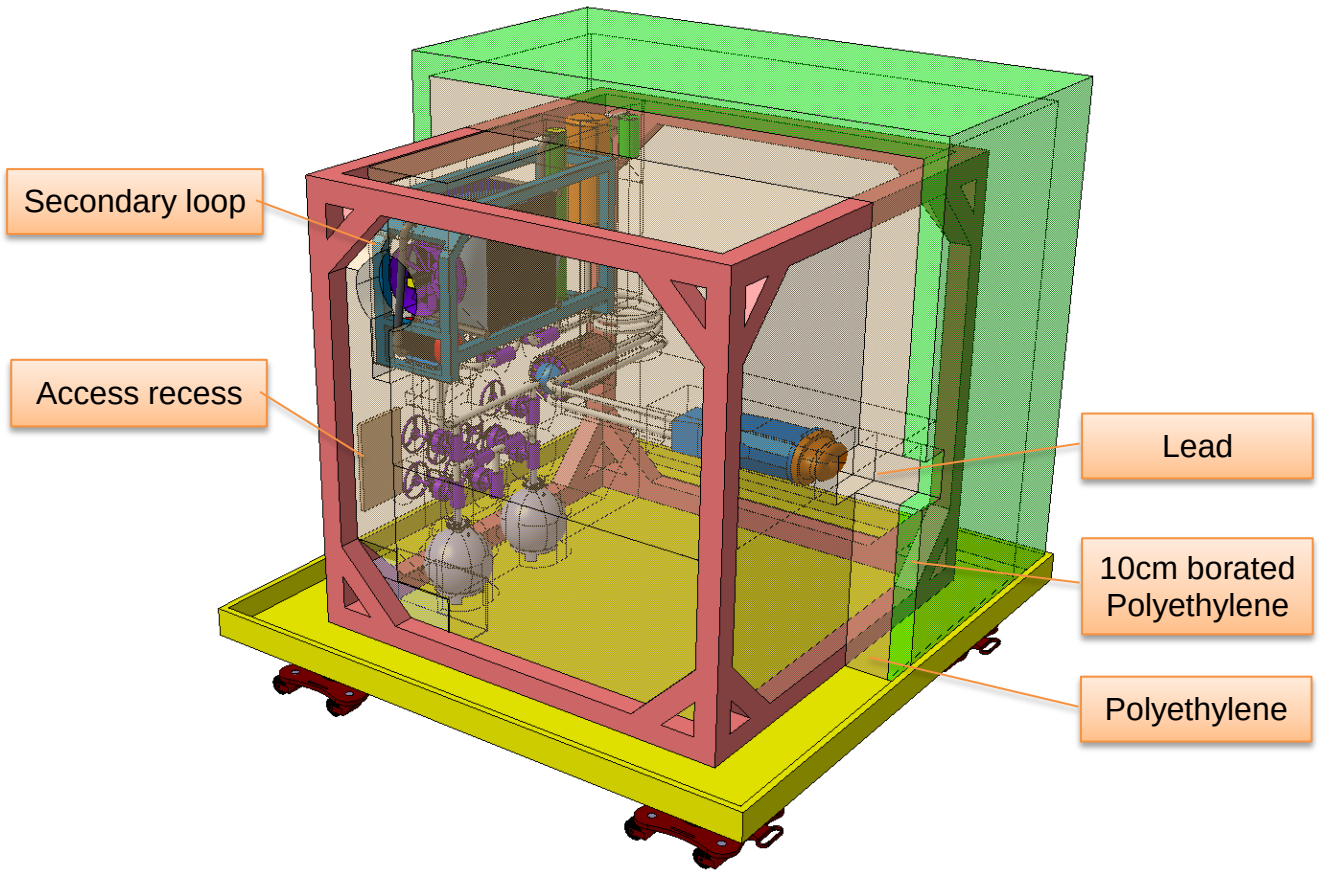

Figure 3: Facility shielding

Note that in the figure above the secondary loop is also shown (refer to subsequent sections)

Special dedicated robotic tools will be necessary to extract the samples from the target. This will entail withdrawing part of the shielding at the front of the facility to allow the dismounting of the target window which once the target is open gives access to the sample holder. The samples contained in the sample holder can then all be removed in one operation to a hot-cell for final manipulation. Thus the parts that need manipulating are fairly large and should not pose a major problem in terms of the robotics needed to handle them. Indeed it is anticipated that standard industrial robots fitted out with the necessary shielding to protect the electronics will be sufficient for this task.

Once the sample holder is removed, a new sample holder with fresh samples can be mounted, the target window replaced and the target closed. The front beam tube in the facility will then be “plugged” with a dummy lead/polyethylene insert to decrease the environmental doses sufficiently to allow access for manual maintenance of the remainder of the facility.

1.3 The spallation target and sample loading

The target is the focus of extensive investigations in Ref.3 from a fluid dynamic point of view to optimise the flow inside the target and create the best conditions for cooling the beam window and the samples. The current section sums up the current state of the design and refers the reader back to Ref.3 for more details.

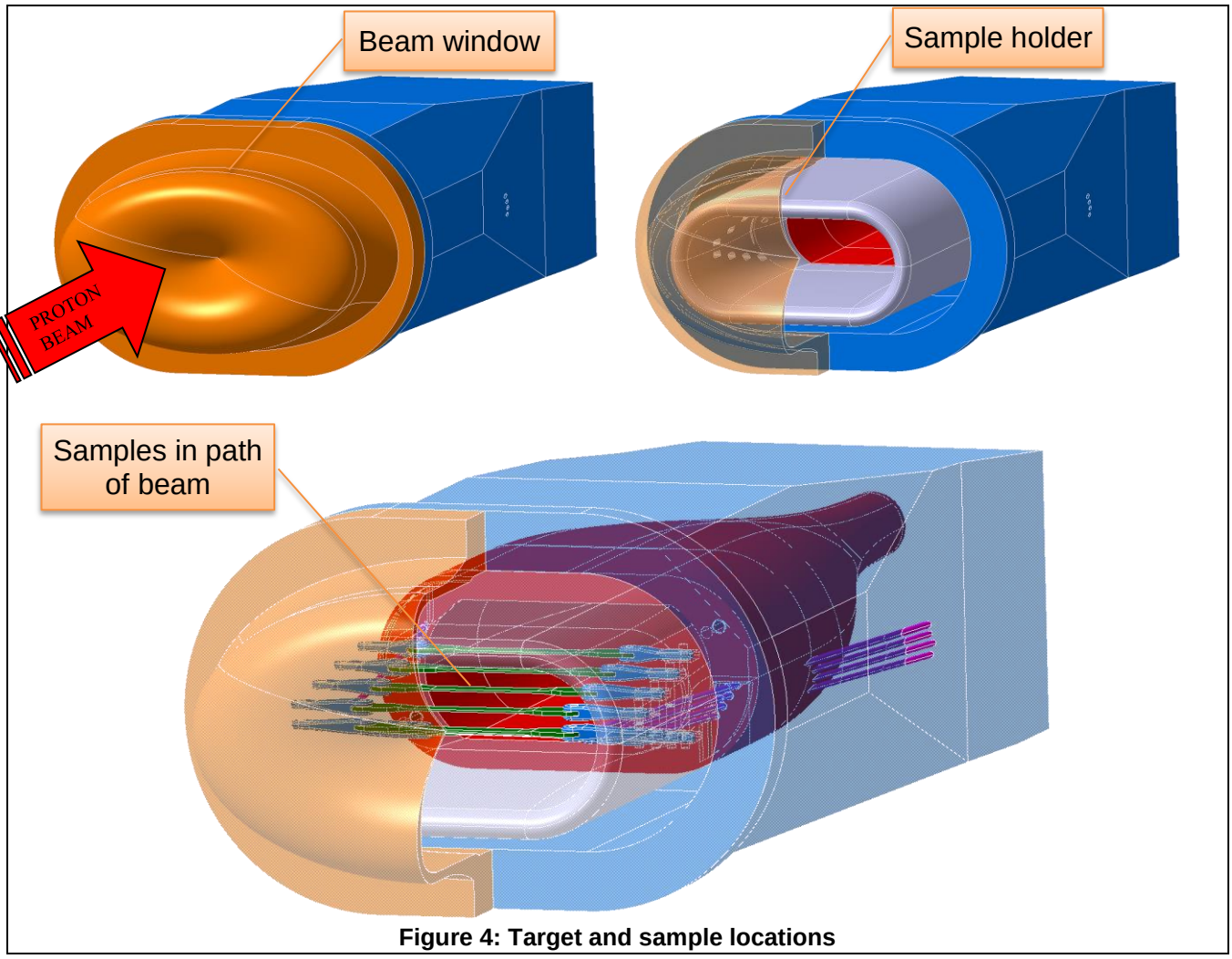

Figure 4: Target and sample locations

Upon impact the beam passes first through the beam window which is cusp shaped and thus optimally cooled by the reversing flow of fluid passing on from the annulus (refer to analysis in Ref.3). The beam then impacts directly the samples imposing DPA from proton interaction. The beam also impacts the surrounding primary fluid, a heavy nuclei, resulting in the production of a large number of spallation neutrons which also contribute to the DPA irradiation damage in the samples.

The samples are held in a sample holder which is an integral form of the internal guide tube through which the fluid flows out of the target towards the heat exchanger. Hence the samples are cooled by the reversing primary fluid. In this manner an environment replicating the use of these materials in fast reactors or ADS type application is created.

The irradiation, temperature and corrosive effects are all represented in the current design. In addition a mechanical system allows a stress to be imposed on the samples, either constant or cyclical. This aspect is particularly important to material embrittlement studies or fatigue studies. The method of applying stress to the samples is illustrated in the next following figures.

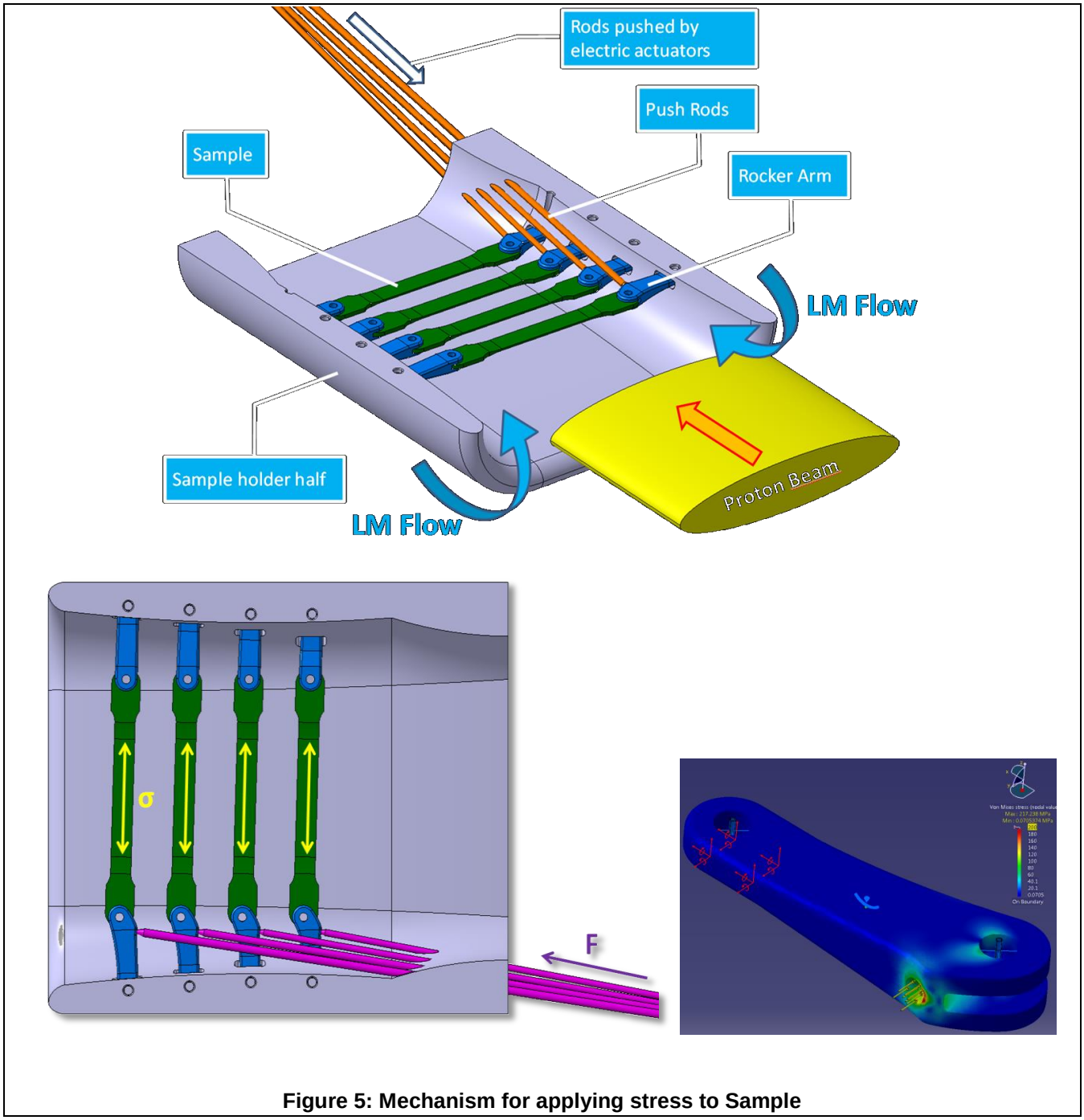

Figure 5: Mechanism for applying stress to Sample

As seen above, push rods are pushed by actuators situated outside the target. The push rods are able to penetrate through dedicated channels isolated by bellows ensuring leak-tightness of the primary circuit. The actuators are themselves located well beyond the maximum neutron flux to preserves their electrical components. Alternately, pneumatic actuators may be used.

The push rods are segmented, one part remaining attached to the target, the other to the sample holder. Since the push rods apply only compression loads, the interface between the two sets of push rods at the interface between the dismountable sample holder is easy to disconnect; the interface being merely a compression face.

The final sets of push rods located in the sample holder then apply a compressive force to a rocker arm which de-multiplies the load into a tensile stress applied to the sample. A relatively modest load from the actuator (~ 850 N) is sufficient to guarantee 500 MPa is attained in the samples.

1.4 Primary loop pressurisation

In order to dampen volume variations in the primary circuit due to the fluctuation of the temperature inside the loop, a pressuriser tank is added at the top of the facility, which can at the same time serve to collect all the hazardous gases resulting from the spallation process in the target.

With this implementation of the pressuriser it is possible to control pressure by simply either bleeding or feeding inert gas into the tank. An alternative method in the case of mercury would be the use of an electric heater to create a mercury vapour however this would create a chemical hazard. The method of pressure control through inert gas is well established and if properly implemented with appropriate venting can be made safe against the leaking of radioactive gases.

In parallel to the venting function, a control of any sudden overpressure must be guaranteed to protect the primary circuit against pressure rupture. Such rapid pressure shocks are always possible in a liquid as a result mainly of power excursions, which are always envisaged as part of the safety cases. A first level of protection is afforded by a spring-loaded valve which evacuate the over pressurized gases up to a certain level, above which a second protection measure in the form of a burst disk takes over should the pressure continue to rise. The first level serves to protect against most anticipated accidental scenarios and has the property of both opening and closing again, which allows the facility to continue to be operational. The second device may only open, hence once that ultimate pressure level has been reached, a total overhaul of the facility is mandatory. Both devices must feature a filtering system to provide some degree of retention of gaseous products, as large as reasonably feasible.

Another function of the pressuriser is to allow the sampling of the gases which are expected to collect at the top of the pressuriser. A dismountable gas sample bottle is therefore foreseen to allow these gaseous spallation products to be collected, analysed and then transported to a treatment plant where they are allowed to decay as the isotopes are usually short-lived before reaching admissible activity levels suitable for their release into the environment.

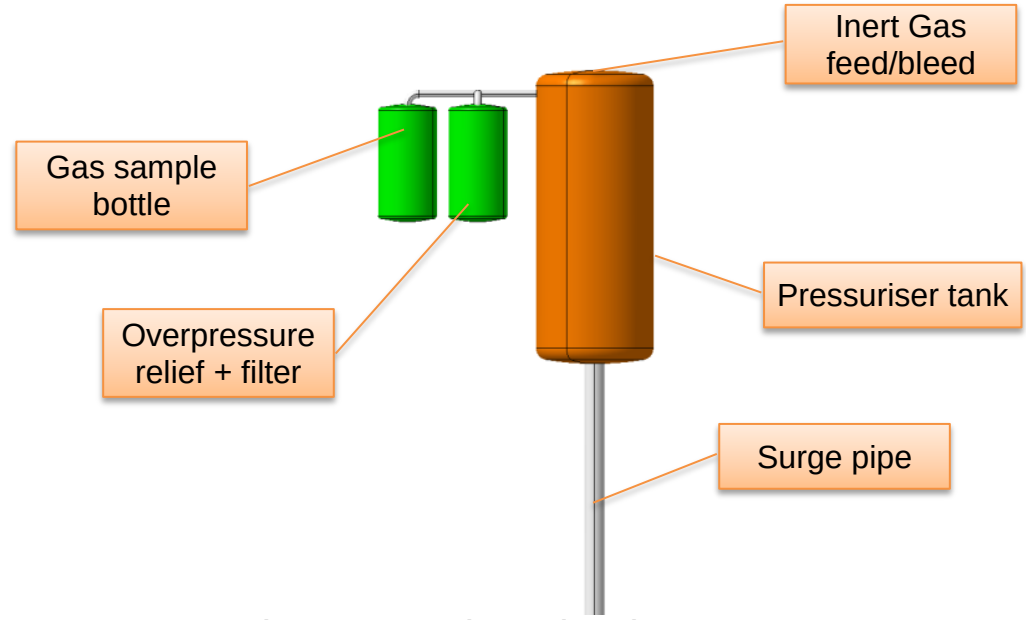

Figure 6: Pressuriser and venting systems

The design study has currently not yet examined these components at great length and they are merely represented in the figure above in terms of their expected volume and position. A deeper analysis of these components will be necessary in the next stage of the project.

1.5 Filtering and cleaning

During the operation of the target impurities are created in the liquid metal in part because of the transmutation effect induced by spallation and also the chemical corrosion caused by oxygen present in the loop. As they tend to concentrate activity they must be regularly withdrawn from the loop by filtering. To avoid it becoming a significant important source of pressure loss during operation, the filter is not inserted on the main route but on a by-pass section.

Whenever considered necessary, an appropriate selection of by-pass valves allows the primary liquid to flow through the filter. Once sufficient activity has been accumulated in the filter, the bypass is closed and the flow returned to normal operation. Regular use of the filter should prevent the deposition of active corrosion products along the walls in the primary circuit which can in the long terms contaminate the facility to such an extent that it can no longer be maintained or relocated to another facility. The filter can be exchanged during shutdown periods, using robotics.

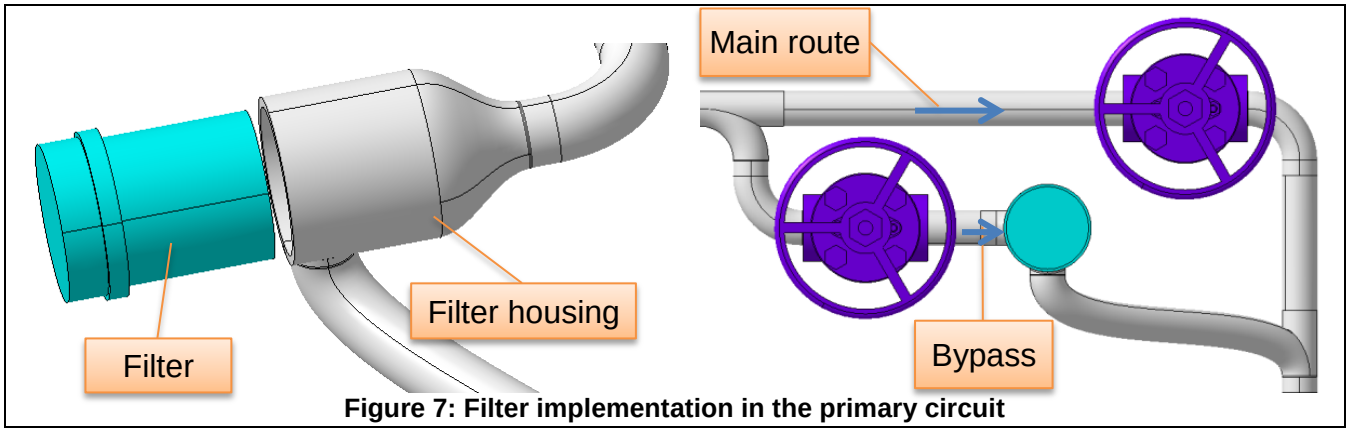

Figure 7: Filter implementation in the primary circuit

1.6 Electromagnetic Pump

In the primary loop, an electromagnetic pump is selected as it contains no moving parts, an important consideration when dealing with a highly radioactive environment in terms of maintenance and reliability. The working principle based on magneto hydrodynamics has a fairly low efficiency, resulting in high power consumption. A flow rate of 1,4 m3/h is required.

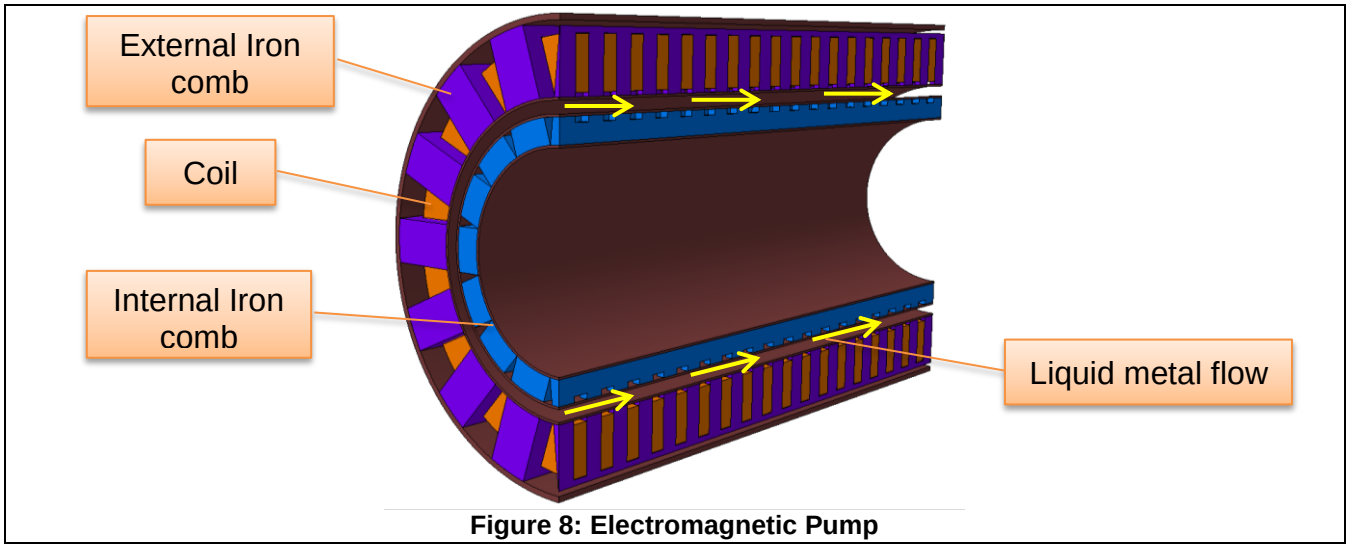

Figure 8: Electromagnetic Pump

1.7 Decay tank

The decay tank collects all the liquid in the primary circuit during the shutdown to allow the opening of the primary circuit in order to access the samples but also to decrease the overall activity around the target area. Sizing the decay tank is directly related to the total volume of liquid in the primary circuit with some margin. The shape giving the greatest capacity with the smallest overall dimensions is a sphere; it's also the optimal configuration for shielding because much of the radioactive fluid is then self-shielded by the surrounding fluid and the total surface irradiating out into the environment is minimised compared to the volume it contains. The decay tank features:

- A main pipe for filling and draining the tank. This pipe must reach the very bottom of the tank to be able to evacuate the totality of the liquid when it is drained by applying over-pressure in the tank compared to the primary circuit.
- Sufficient access in terms of an observation hole to permit inspection using a borescope camera. In the current design the inspection hole stopper are identical and the decay tank would need to be dismounted for inspection.
- A gas plug at the top of the tank to pressurize the tank allowing it to be drained. It can also be used to extract the gases which accumulate in the liquid due to radioactive decay.

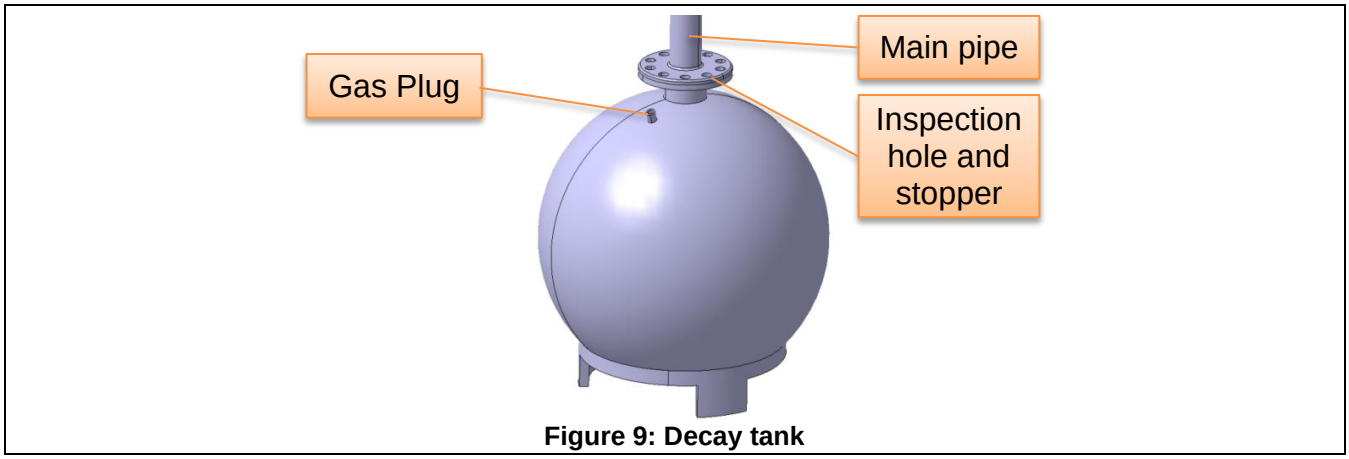

Figure 9: Decay tank

There are two decay tanks in the facility for reasons of safety, notably redundancy and operational maintenance since it allows fresh liquid to be pumped into the primary circuit while the used fluid is allowed to decay. An external interface also allows evacuation of the liquid for external disposal. A series of valves allows redundancy in operation and exchange of fluids.

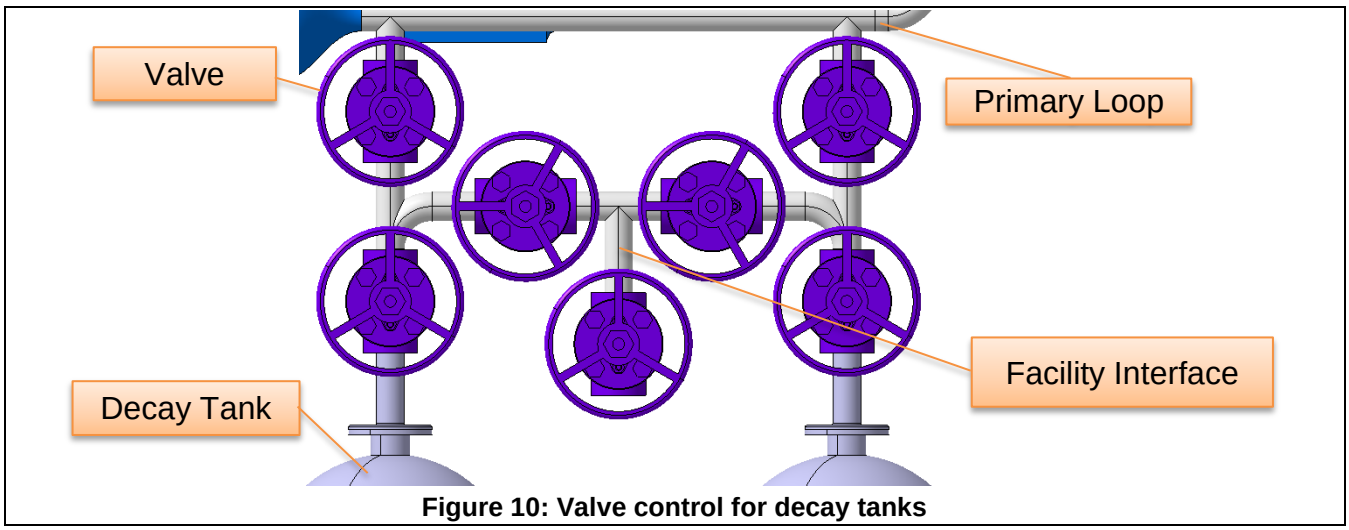

Figure 10: Valve control for decay tanks

1.8 Heat Exchanger

The design of the heat exchanger is explained at greater length as the design is somewhat novel featuring a dismountable interface between the primary and secondary side.

1.8.1 Design concept of the heat exchanger

The heat exchanger design is addressed in section 2.2.1 of Ref.2 and a broad concept is proposed which features a central pin containing the primary fluid centrally located inside an outer spiral containing the secondary fluid. The spiral shape permits to extend the path length, therefore the efficiency increases and the volume stays compact. The two components are in thermal contact but are physically distinct, having no common wall as is often the case in traditional heat exchangers.

The concept is summed up in figure 11 below.

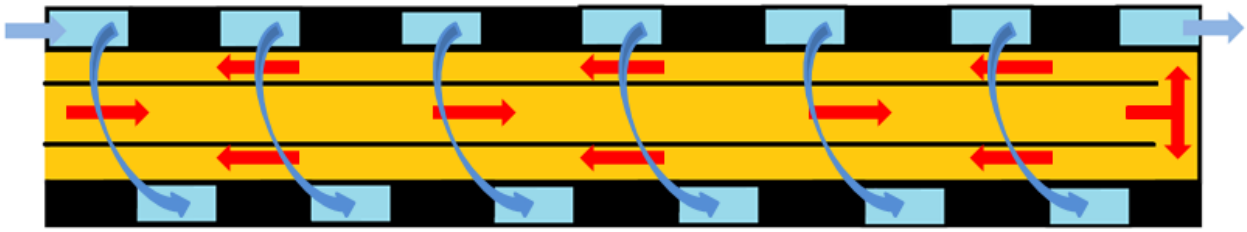

Figure 11: Heat Exchanger concept for T-MIF

A primary-side (orange) pin is inserted inside a secondary-side (blue) barrel with a spiral flow

The main advantage of this arrangement is its inherent safety. The two sides can be disassembled easily from one another by removing the pin from the barrel since the two are not attached.

Furthermore the small gap between the external wall of the primary-side pin and the secondary-side spiral-flow barrel can be filled with a thermally conductive gas which in the event of a leak from either side will catch the leaking fluid without breaking through to the other side, thus preventing contamination from the primary fluid from reaching the secondary circuit. In addition the leak will provoke an immediate rise in the gas pressure of the interface gap, a very robust leak detection device which was proven to work quite well both in the safety test of MEGAPIE and in the MEGAPIE test itself.

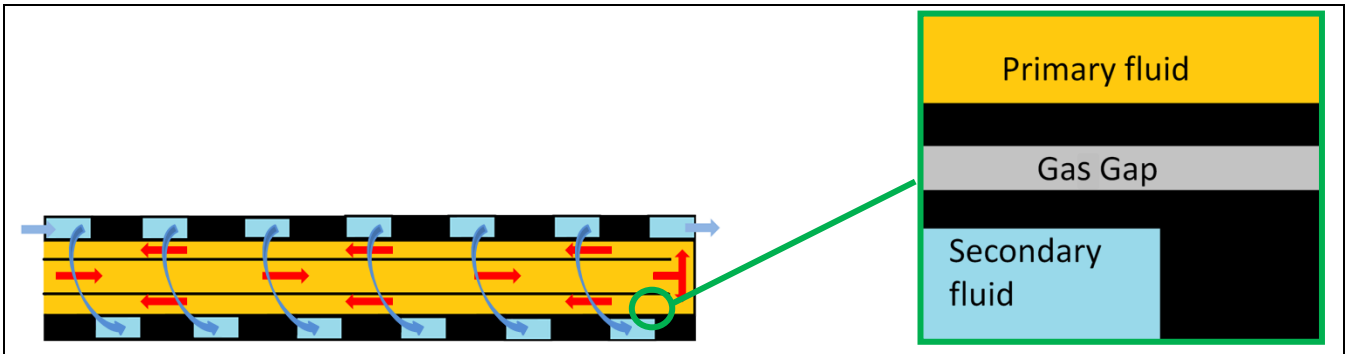

Figure 12: Interface primary / secondary circuit through heat exchanger

1.8.2 One dimensional Calculations of the heat exchange

The initial design of the heat exchanger has been optimised using one dimensional theory in which both fluids are considered as circulating in conformal tubes

1.8.2.1 Theory

In order to gain a first insight into the performance of the heat exchanger, simple one-dimensional calculations are performed using the LMTD method (Log Mean Temperature Difference). This method computes the exchanged power and subsequently the necessary exchange surface based on the in- and output temperature of both primary heater-side and secondary cooling fluids.

According to the primary specifications for this heat exchanger, liquid metal fluids are used such as Lead, Lead-Bismuth Eutectic and Gallium, the exchanged power will be approximately 100 kW and temperatures on the primary side should not exceed 600°C to avoid Polonium evaporation from the LBE in the target. Obviously, the considered range of temperature needs to reflect the fact that the metals must remain in their liquid state.

Thus, the process envisaged is to create an Excel sheet following the LMTD method from which the in- and output temperatures of both fluids may be derived to obtain the required heat exchange. From this configuration, the exchange surface and then the exchanger dimensions may be deduced.

1.8.2.2 Fluid properties

Before starting any calculation, some characteristics of the potential fluids used in the thermal exchanger must be collated. Indeed, these potential fluids that best fit the desired configuration are Gallium, Lead and Lead-Bismuth Eutectic and the needed characteristics are:

- Maximum and minimum operational temperatures (T°) that will a liquid state.
- Density (ρ)
- Specific heat capacity (C_p)
- Thermal conductivity (λ)
- Dynamic viscosity (μ)
- Molar mass (M)

Fluid:	Gallium			
Inlet T°	T_e	Min 30	°C	http://jpcrd.aip.org/resource/1/jpcrbu/v41/i3/p033101_s1
Outlet T°	T_s	Max 1227	°C	
Density	ρ	6033	kg/m3	
Specific heat capacity	C_p	381	J/(kg.K)	At 373 °K
Thermal conductivity	λ	41	W/(m.K)	
Dynamic viscosity	μ	0.001263	Pa.s	
Molar Mass	M	69.723	g/(mol)	

Fluid:	Lead			
Inlet T°	T_e	Min 327.46	°C	http://www.oecd-nea.org/science/reports/2007/pdf/
Outlet T°	T_s	Max 1027	°C	
Density	ρ		kg/m3	*11367-(1,1944.T)*
Specific heat capacity	C_p		J/(kg.K)	*175,1-(0.04961.T)+(0.00001985.T^2)-(0.000000002099.T^3)-(1524000.T^-2)*
Thermal conductivity	λ		W/(m.K)	*9,2+(0,011.T)*
Dynamic viscosity	μ		Pa.s	*0,000455.exp(1069/T)*
Molar Mass	M	207.2	g/(mol)	

Fluid:	Lead-Bismuth Eutectic			
Inlet T°	T_e	Min 130	°C	http://www.oecd-nea.org/science/reports/2007/pdf/
Outlet T°	T_s	Max 1000	°C	
Density	ρ		kg/m3	*11096-(1,3236.T)*
Specific heat capacity	C_p		J/(kg.K)	*159-(0,0272.T)+(0,00000712.T^2)*
Thermal conductivity	λ		W/(m.K)	*3,61+(0,01517.T)-(0,000001741.T^2)*
Dynamic viscosity	μ		Pa.s	*0,000494.exp(754,1/T)*
Molar Mass	M	208.21	g/(mol)	

Table 2: Calculation sheet extract - Fluids properties

In addition, the thermal conductivity (λ_p) and the roughness index (k) of the Stainless Steel that will be used as the piping material are also needed.

Material	Stainless steel		
Thermal conductivity	λ_p	60.5	W/(m.K)
Roughness index	k	0.1	mm

Table 3: Calculation sheet extract - Material properties

1.8.2.3 Simplified calculation for scoping analysis

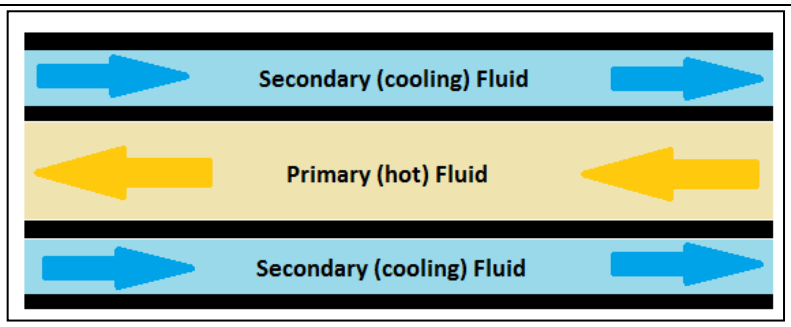

Figure 13: Initial simplified model

In a first calculation, the heat exchanger is represented by 2 concentric pipes, the primary fluid flowing through the inner pipe and the secondary (or cooling) fluid flowing counter-current through the outer pipe as represented above. However, it should be borne in mind that these results relate to an ideal concentric tube model and do not take into account every parameter of the real configuration. However it gives a good first approach of the exchanger specifications and the fluids conditions, which is to be completed by a 3D model later in the analysis.

The following simulation uses LBE as the primary fluid due to its wide liquid state temperature range and Gallium as the secondary fluid for its superior conductivity properties.

Primary fluid:	LBE		
Inlet T°	T_{e1}	550	°C
Outlet T° $T_{s1} < T_{e1}$	T_{s1}	300	°C
Volumetric flow rate	Q_1	1	m3/h
Density	ρ_1	10171.92866	kg/m3
Specific heat capacity	C_{p1}	143.4807036	J/(kg.K)
Thermal conductivity	λ_1	13.35234873	W/(m.K)
Dynamic viscosity	μ_1	0.001454876	Pa.s
Prandtl's number $\mu_1.C_{p1}/\lambda_1$	Pr_1	0.015634	
Mass flow $Q_1.\rho_1$	m_1	2.825536	kg/s
Flow capacity $m_1.C_{p1}$	C_1	405.409856	J/(s.K)

Secondary fluid:	Gallium		
Inlet T°	T_{e2}	75	°C
Outlet T° $T_{s2} > T_{e2}$	T_{s2}	120	°C
Volumetric flow rate $m_2.\rho_2$	Q_2	3.527492	m3/h
Density	ρ_2	6033	kg/m3
Specific heat capacity	C_{p2}	381	J/(kg.K)
Thermal conductivity	λ_2	41	W/(m.K)
Dynamic viscosity	μ_2	0.001263	Pa.s
Prandtl's number $\mu_2.C_{p2}/\lambda_2$	Pr_2	0.011737	
Mass flow	m_2	5.911488	kg/s
Flow capacity $m_2.C_{p2}$	C_2	2252.28	J/(s.K)

Exchange surface:	Stainless steel		
Thermal conductivity	λ_p	60.5	W/(m.K)
Wall thickness	e	5	mm

Fluid average T° 1	T_{moy1}	425	°C
Fluid average T° 2	T_{moy2}	97.5	°C

Exchanged power $C_1(T_{e1}-T_{s1})=C_2(T_{s2}-T_{e2})$	ϕ	101352.463943	W	≈ 100kW
Mass flow $\varphi/(C_{p2}.(T_{s2}-T_{e2}))$	m_2	5.911488	kg/s	
Flow capacities ratio C_1/C_2	R	0.18		
Exchanger efficiency $(T_{e1}-T_{s1})/(T_{e1}-T_{e2})$	ε	0.526316		
> According to Kern's literature, corrective coef	F	0.97		

The green cells are the input data needed to drive the computation; they are the only parameters to be modified. The grey cells are taken from the materials properties seen above; the values depend on the fluid average temperatures. All the other cells of this sheet are computed and cannot be manually changed.

The exchanged power is directly linked to the working temperatures and current settings lead to a value close to the required 100 kW.

Table 4: Heat Exchanger results with LBE

In the configuration shown, an exchanged power close to 100kW is reached, within temperatures limitations. Thus almost all the information needed is available for a final calculation of the exchanger specifications. Beforehand, the pipes diameters must be chosen.

Exchange pipe 1's diameter	D_1	0.025	m
Exchange hydraulic diameter 1	D_{h1}	0.025	m
Exchange hydraulic flow area 1	A_1	0.000491	m2
Exchange pipe 2's diameter	D_2	0.05	m
Exchange hydraulic diameter 2	D_{h2}	0.02475	m
Exchange hydraulic flow area 2	A_2	0.000481	m2

The hydraulic diameter is obtained by computing 4*area/perimeter. The hydraulic area is then derived from the hydraulic diameter.

Table 5: Heat Exchanger dimensions with LBE

Logarithmic average T° $(Te1-Ts2)-(Ts1-Te2)/ln((Te1-Ts2)/(Ts1-Te2))$	ΔT_{ML}	316.51	°C
Fluid velocity 2 Q_2/A_2	v_2	2.036266	m/s
Reynolds' number 2 $\rho_2.v_2.D_2/\mu_2$	Re_2	240759.857448	
Colburn's correlation > exchange coef $(\lambda_2/D_2).0,023.(Re_2\text{^}0,8).(Pr_2\text{^}(1/3))$	h_2	174853.474138	W/(m2.K)
Fluid velocity 1 Q_1/A_1	v_1	0.565884	m/s
Reynolds' number 1 $\rho_1.v_1.D_1/\mu_1$	Re_1	98911.084371	
Nusselt's number 1 $0,36.(Re_1\text{^}0.55).(Pr_1\text{^}(1/3))$	Nu_1	50.316199	
Exchange coef $\lambda_1.Nu_1/D_1$	h_1	26873.577352	W/(m2.K)
Global exchange coef inverse $1/(h_1.(D_1/D_2))+(1/h_2)+(D_2/2.\lambda_P).ln(D_1/D_2)$	1/K	0.000045	
Then	K	22422.991856	W/(m2.K)
Exchanger's surface $\varphi/(F.K.\Delta T_{ML})$	S	0.014722	m2
Exchanger length	L	0.133893949	m

From the 2 flows specifications and the piping dimensions, both fluids velocities are obtained and subsequently their Reynolds' numbers.

The aim of this sheet is to obtain the global power exchanged to finally derive the heat exchanger dimensions.

Table 6: Heat Exchanger specifications with LBE

The configuration with LBE above ties in well with project needs from a thermal-hydraulic point of view. Liquid LBE as a primary fluid enters the inner part of the exchanger at 550°C at 1 m^3/h and exits at 300°C. On the secondary side liquid Gallium as a cooling fluid enters the outer part of the exchanger at 75°C and approximately 3.5 m^3/h and leaves at 120°C. In the actual configuration, the LBE needs to share 0.0147 m2 with the Gallium to shed the100 kW deposited by the beam in the target.

However, after discussion with the management of the PSI Hotlab, a consensus was reached to replace LBE by Lead as the primary fluid, to avoid any production of polonium which would impose a higher classification of the laboratory where the facility may be positioned. Since lead will freeze at a higher temperature than LBE, the temperature range of the primary side exchanger needs to be adapted. Hence, instead of cooling the primary fluid down to 300°C, a minimum of 380°C is chosen; 327°C being the solidification temperature of lead.

A repeat of the calculations with the tables above yields the following results

Primary fluid:	Lead		
Inlet T°	T_{e1}	550	°C
Outlet T° $T_{s1} < T_{e1}$	T_{s1}	380	°C
Volumetric flow rate	Q_1	1.4	m3/h
Density	ρ_1	10485.35364	kg/m3
Specific heat capacity	C_{p1}	145.6547343	J/(kg.K)
Thermal conductivity	λ_1	17.31965	W/(m.K)
Dynamic viscosity	μ_1	0.001936258	Pa.s
Prandtl's number $\mu_1.C_{p1}/\lambda_1$	Pr_1	0.016284	
Mass flow $Q_1.\rho_1$	m_1	4.077638	kg/s
Flow capacity $m_1.C_{p1}$	C_1	593.927211	J/(s.K)

Secondary fluid:	Gallium		
Inlet T°	T_{e2}	75	°C
Outlet T° $T_{s2} > T_{e2}$	T_{s2}	120	°C
Volumetric flow rate $m_2.\rho_2$	Q_2	3.514098	m3/h
Density	ρ_2	6033	kg/m3
Specific heat capacity	C_{p2}	381	J/(kg.K)
Thermal conductivity	λ_2	41	W/(m.K)
Dynamic viscosity	μ_2	0.001263	Pa.s
Prandtl's number $\mu_2.C_{p2}/\lambda_2$	Pr_2	0.011737	
Mass flow	m_2	5.889042	kg/s
Flow capacity $m_2.C_{p2}$	C_2	2243.73	J/(s.K)

Exchange surface:	Stainless steel		
Thermal conductivity	λ_p	60.5	W/(m.K)
Wall thickness	e	3	mm

Fluid average T° 1	T_{moy1}	465	°C
Fluid average T° 2	T_{moy2}	97.5	°C

Exchanged power $C_1(T_{e1}-T_{s1})=C_2(T_{s2}-T_{e2})$	ϕ	100967.625800	W	≈ 100kW
Mass flow $\varphi/(C_{p2}.(T_{s2}-T_{e2}))$	m_2	5.889042	kg/s	
Flow capacities ratio C_1/C_2	R	0.26		
Exchanger efficiency $(T_{e1}-T_{s1})/(T_{e1}-T_{e2})$	ε	0.357895		
> According to Kern's literature, corrective coef	F	0.97		

Table 7: Heat Exchanger results with Lead

Exchange pipe 1's diameter	D_1	0.025	m
Exchange hydraulic diameter 1	D_{h1}	0.025	m
Exchange hydraulic flow area 1	A_1	0.000491	m2
Exchange pipe 2's diameter	D_2	0.05	m
Exchange hydraulic diameter 2	D_{h2}	0.02511	m
Exchange hydraulic flow area 2	A_2	0.000495	m2

Table 8: Heat Exchanger dimensions with Lead

Logarithmic average T° $(Te1-Ts2)-(Ts1-Te2)/ln((Te1-Ts2)/(Ts1-Te2))$	ΔT_{ML}	363.93	°C
Fluid velocity 2 Q_2/A_2	v_2	1.971393	m/s
Reynolds' number 2 $\rho_2.v_2.D_2/\mu_2$	Re_2	236443.440552	
Colburn's correlation > exchange coef $(\lambda_2/D_2).0,023.(Re_2\text{^}0,8).(Pr_2\text{^}(1/3))$	h_2	169896.401187	W/(m2.K)
Fluid velocity 1 Q_1/A_1	v_1	0.792238	m/s
Reynolds' number 1 $\rho_1.v_1.D_1/\mu_1$	Re_1	107254.491972	
Nusselt's number 1 $0,36.(Re_1\text{^}0.55).(Pr_1\text{^}(1/3))$	Nu_1	53.327014	
Exchange coef $\lambda_1.Nu_1/D_1$	h_1	36944.208521	W/(m2.K)
Global exchange coef inverse $1/(h_1.(D_1/D_2))+(1/h_2)+(D_2/2.\lambda_p).ln(D_1/D_2)$	1/K	0.000032	
Then	K	31083.695473	W/(m2.K)
Exchanger's surface $\varphi/(F.K.\Delta T_{ML})$	S	0.009202	m2
Exchanger length	L	0.094482056	m

Table 9: Heat Exchanger specifications with Lead

The configuration with Lead above ties in also well with project needs from a thermal-hydraulic point of view. Liquid Lead as a primary fluid enters the inner part of the exchanger at 550°C at 1,4 m^3/h and exits at 380°C. On the secondary side liquid Gallium as a cooling fluid enters the outer part of the exchanger at 75°C and approximately 3.5 m^3/h and leaves at 120°C. In the actual configuration, the Lead needs to share 0.0092 m2 with the Gallium to shed the100 kW deposited by the beam in the target.

1.8.3 Heat exchanger Design in 3D using CFD

1.8.3.1 HEX Design

As mentionned in the design concept of the heat exchanger, the actual heat echanger model will be more complex than the one used in the Excel sheet calculation. The primary and secondary part of the exchanger must be simple to assemble, for easy maintenance and to improve security. Thus both the in-and outlet of the primary side are at the same location, in the form of two concentric pipes.

Figure 14: Primary part of the exchanger – sectional view

Furthermore, the secondary fluid flows in a spiral pipe wrapped around the central primary fluid barrel. The part shown in is basically a cylinder that close the upper spiral surface shown in orange.

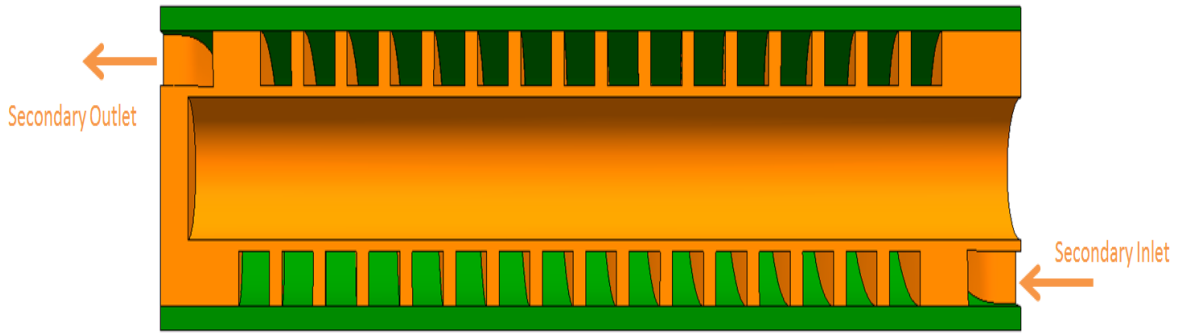

Figure 15: Secondary part of the exchanger – sectional view

Hence primary and secondary parts are fully independent and can be isolated in an emergency or for maintenance. Indeed the exchanger can be easily disassembled by sliding the inner primary part out of the outer secondary part.To improve the exchange efficiency, the fluids are running counter-current along almost the entire exchange surface. A wall at the extremity permit to close the volume between the 2 parts of the exchanger. It prevents an unexpected leak from the primary canal to flow down out of the securized volume and contains the gas used for leak detection.

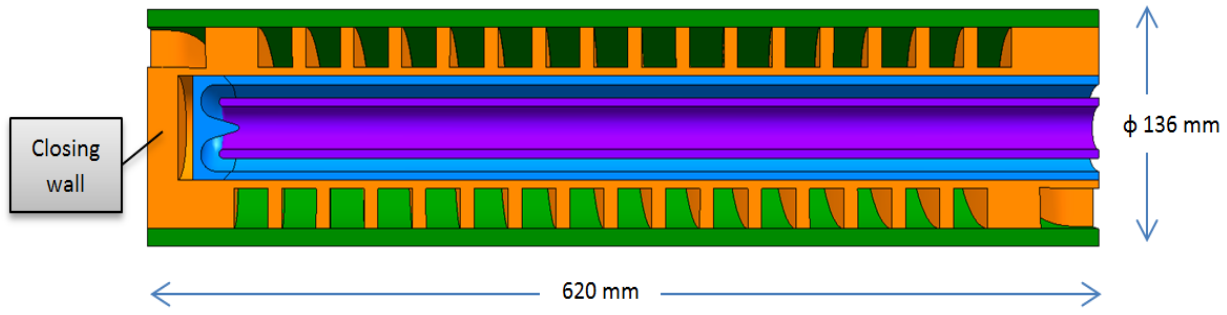

Figure 16: Complete Heat Exchanger – sectional view

This design construction differs slightly from the one used in the Excel simulation. And hence dimension s will differ slightly. Thus the pipe hydraulic flow areas are the same but the diameters are larger. Hence the heat exchange is less efficient than expected. Therefore, in a first instance a longer exchange surface (approximately 500 mm) is set and the resulting heat exchange is checked in a CFD analysis. Then, through iterations, this length may be adapted to the desired specified perofrmance of 100 kW, since the heat exchanged will be roughly proportional to the length.

1.8.3.2 CFD Analysis

In the CFD analysis, excluding the secondary fluid velocity, all the input parameters are from the Excel calculation. Indeed for the secondary fluid velocity, as the spiral path is longer and the walls drag more important, it has been forced at 4 m/s instead of 2 m/s at the in- and outlet. In a first

calculation, only the heat flux is monitored, the outer wall in contact with the environment is taken as adiabatic.

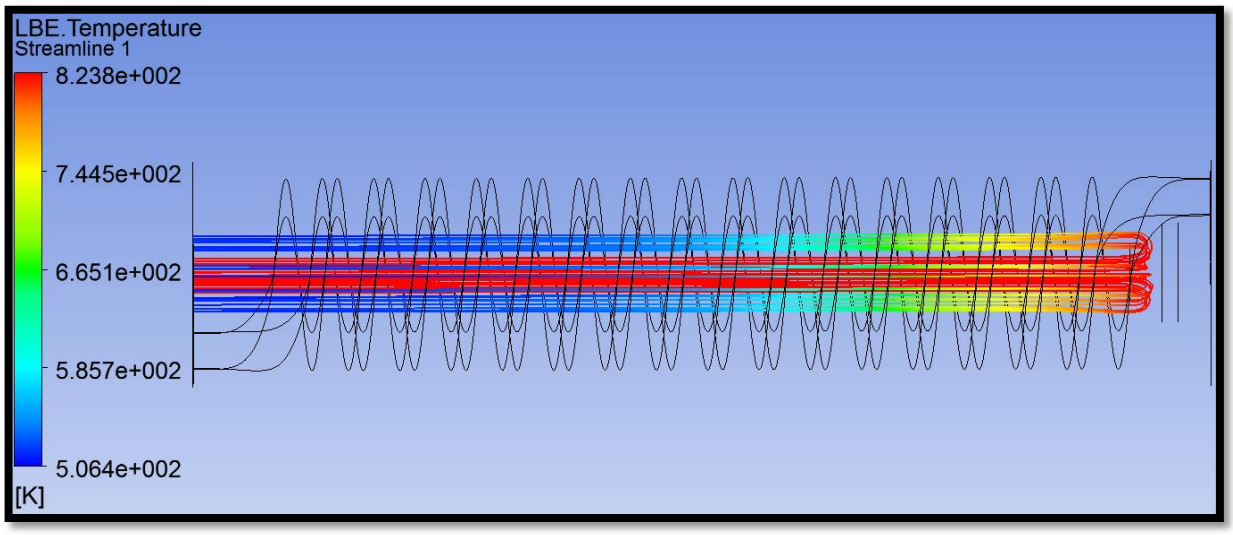

Figure 17: LBE temperature in primary circuit

On the CFD result above, the temperature variation in the primary fluid (LBE) is shown. The inlet temperature is set at 550°C (823°K - 273 = 550°C). The temperature is fairly constant in the first part of the channel because there is no contact with a cold source but it is clear that the LBE cools down along its way back down the outer annulus due to the proximity with the spiral. The LBE leaves the exchanger at a temperature of 233°C. This means the exchanged power is about 130 kW instead of the required 100kW.

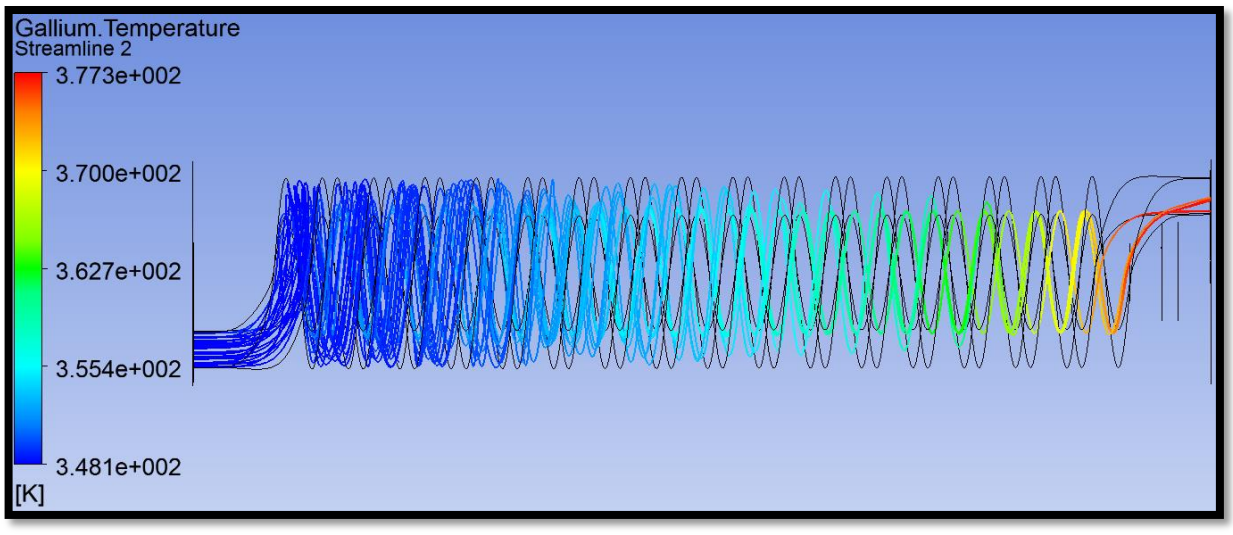

Figure 18: Gallium temperature in secondary circuit

In the figure above the secondary fluid temperature variation along the Gallium flow is shown. As set, the inlet temperature is 75 °C. The heat exiting the LBE warms up the Gallium up and finally reaches the outlet at 104°C.

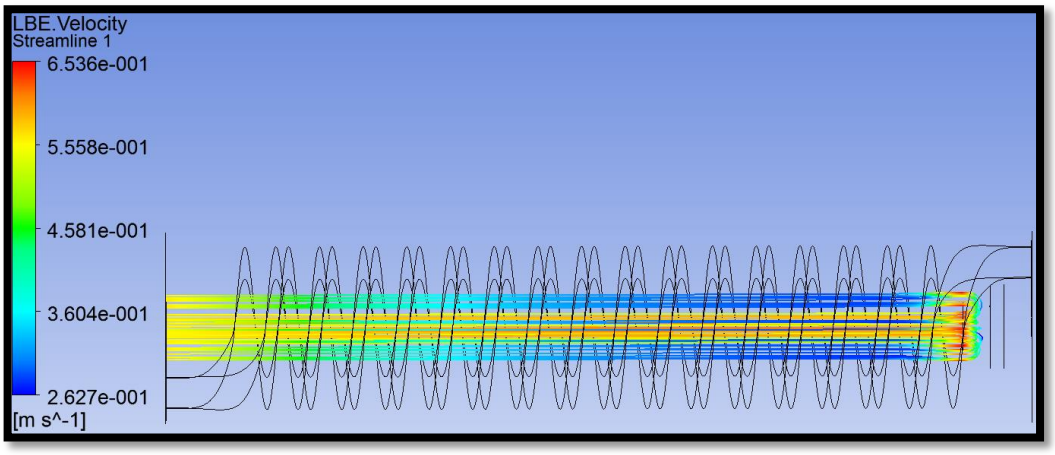

Figure 19: LBE velocity in primary circuit

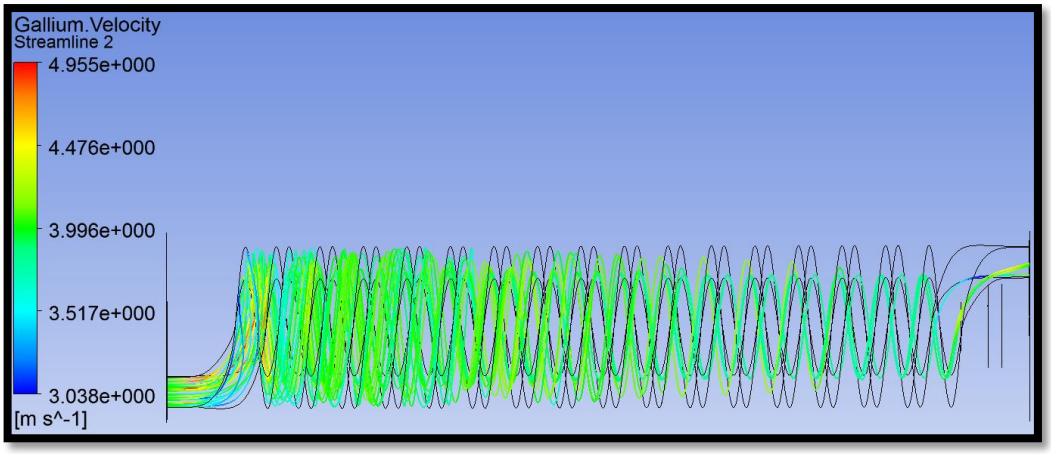

Figure 20: Gallium velocity in secondary circuit

By examining the velocity, it seems the secondary fluid flow is quite constant; the primary fluid tends to slow down after the turn back. It seems to speed up again before the outlet probably due to a homogenous velocity boundary condition.

In conclusion the primary fluid is cooled down more than needed. This means that there is enough scope for reducing the dimensions of the heat exchanger or including a small gas gap between the two parts which would lower efficiency but increase safety by separating the boundaries of the primary and secondary containments. Such a small gas-filled gap between primary and secondary containments would serve both as a barrier and a leak detection device.

1.8.3.3 Variation study of the gap width

The previous calculations demonstrated an increase in exchanged power beyond 100 kW. It may therefore be possible to implement a gap between the spiral and the pin, which will have several effects:

- Adds thermal resistance. Hence thermal performance is degraded. This may be acceptable since the previous calculation showed the target of 100 kW was exceeded.

- Acts as buffer to prevent a crack from the primary side form propagating into the secondary side. If the gap is sufficient, there will be no direct contact between the two and hence no thermal stresses.

- Acts as a leak detection device, any leak provokes an increase in pressure.

- Allows to control the direction of the leak by managing the pressure in each circuit. For instance if $P_{secondary} > P_{gas} > P_{primary}$, then radioactive volatiles will remain confined in the event of any breach of the containments. The strategy of stratifying the pressure levels is used with success in conventional nuclear power plants to prevent leaks of radioactivity during operation and minor deviations.

The first simulations show that the heat exchanged between the two parts becomes almost insignificant as soon as the two surfaces are physically completely separated, even if this gap is filled by a conductive gas such as Helium and reduced to a minimum, constrained by manufacturing tolerances.

Since the advantages listed above seem desirable, an alternative design has been sought which conserves these desirable properties whilst enabling the flow of heat.

1.8.3.4 Inlaid copper conduction strap

A new component is needed in order to insure a good heat contact between the primary and the secondary containment while conserving the gas gap. This new component is a highly conductive copper strap inserted between the two containments. However, to keep the same exchange surface and the same exchanged power of 100kW, the heat exchanger flow needs to be increased as the contact surface decreases.

After several simulations of gas thermal exchange, it seems adequate to assume that the whole power of 100kW is transferred by the copper strap and that the gas conduction may be neglected in the simulations. The copper strap is coiled inside the gas gaps and has the additional advantage of aiding in correctly positioning the primary inside the secondary.

As a first test to ensure good thermal contact between the primary and secondary parts of the exchanger, a simulation is carried with a simple spiral wire. This wire is 1mm in diameter and is rolled up around the pin like a spring. This solution proves to be not efficient enough, because of the very small contact surface between the cylinder and a plane, as shown below.

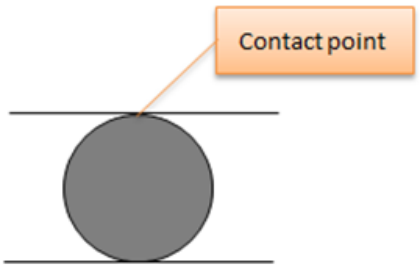

Figure 21: spiral wire in the gas gap

Hence, in the next attempt, the circular section is replaced by a rectangular section, more like a strap (2mm x 0,8mm) to increase thermal contact. This configuration is much more efficient but computations show the exchanged power still needs to be improved. Another design is tested, represented by straight rectangular (1,5mm x 0.5mm) lamellas parallel to the axis of the containment cylinder, in order to observe the effect of the orientation of the material on the exchange efficiency. It appears that the exchange is thus significantly improved, even with a smaller total contact surface.

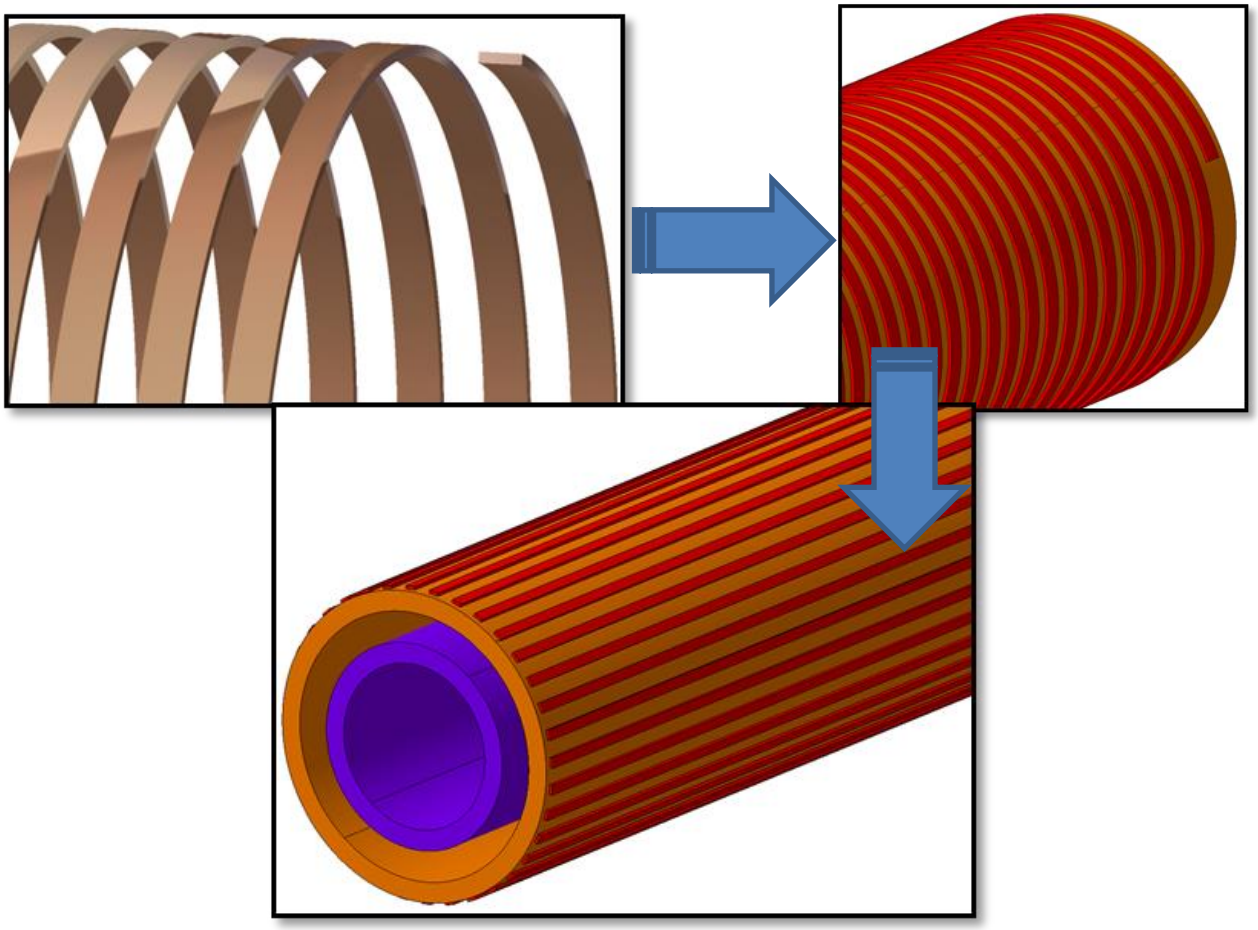

Figure 22: improved conductance strap

These lamellas are a valid thermal design but would be difficult to align in a real design, particularly if the two containments are to be separated for maintenance. A corrugated copper sheet concept (0,2mm thickness) is proposed as a feasible design which conserves this lamellas heat exchange properties. The corrugated cylindrical sheet can be placed in the gap materialising a good thermal contact surface between the primary and the secondary containments of the heat exchanger. It also ensures to a fair degree that both components be well located coaxially. The small thickness of the sheet and the small stiffness of the copper allow it to be deformed by differential thermal expansions without producing too much stress while keeping an optimum thermal contact. This final variant is kept for the next optimization simulations.

1.8.3.5 CFD Analysis with corrugated copper sheet in gas gap

The same calculations are repeated, assuming the modified design as described previously. The effect of the heat exchange is documented in the figures hereafter. The primary fluid constituted now by Lead (Pb) which replaces the LBE, enters the heat exchanger at 550°C and its' outlet mean temperature reaches 377°C. The lead flows at a fairly constant velocity of 0.8 m/s.

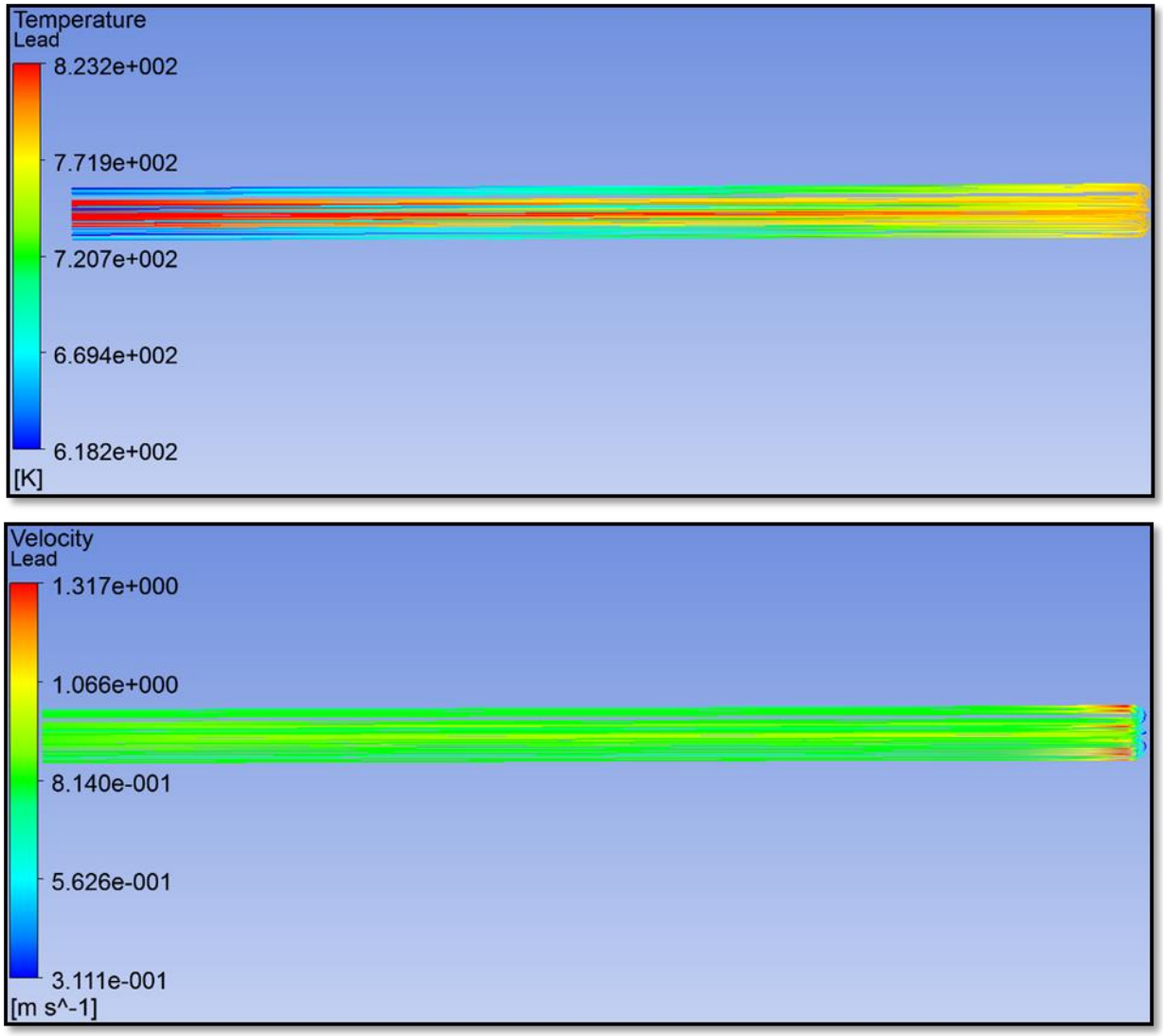

Figure 23: Liquid Lead temperature and velocity in primary circuit

On the secondary side, Gallium enters the spiral at 75°C and exits at a mean value of 119°C. The gallium passes through the spiral at a fairly constant velocity with an average of 2,9 m/s.

In this configuration, the heat exchanger is able to extract 100kW from the primary fluid and thus fully matches its specifications.

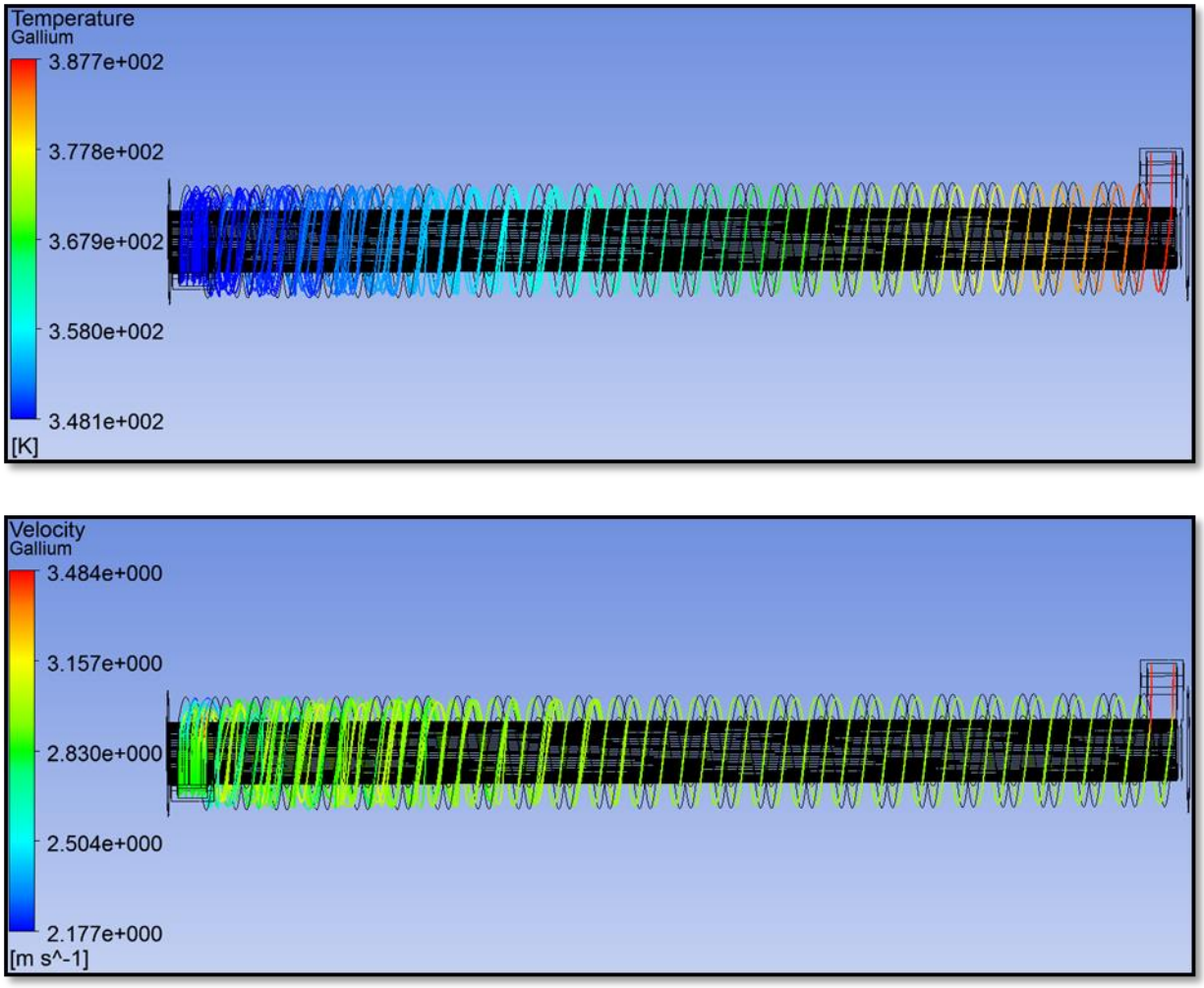

Figure 24: Liquid Gallium temperature and velocity in secondary circuit

2 Overall layout of the secondary loop

The secondary loop is an entirely removable component, which interface with the primary via the primary heat exchanger. The interface constituted by a hollow barrel which slots over the pin of the primary circuit allows the extraction of the entire secondary loop which is located inside a separate truss.

The heat that is extracted by the gallium from the primary loop is passed on to a secondary fin-type heat exchanger which is simply air cooled. There is therefore no need for any connection to the cold source, which is essentially the air of the lab. This air will have to be cooled by the environmental systems of the lab. These systems need to be dimensioned so as to cope with the extra 100 kW. This is a conservative figure, given that in reality only 70% of the 100 kW beam is dumped as heat, the remaining 30% are extracted by the energy of the escaping neutrons.

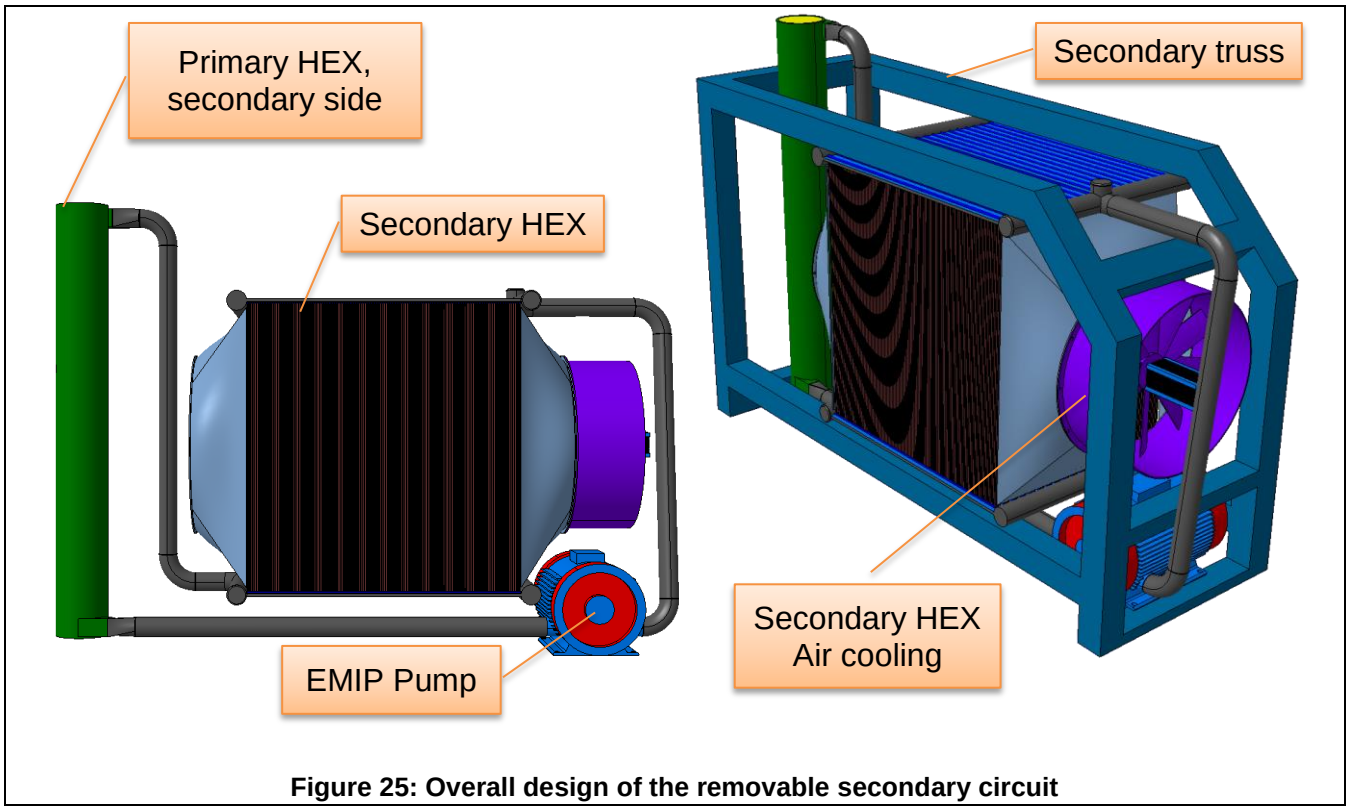

Figure 25: Overall design of the removable secondary circuit

The secondary loop has been sketched out in its most important aspects, however not with the degree of detail of the primary circuit. The heat exchanger, air circulation system and pump are examined.

In addition, the control systems for regulating the flow and secondary pressure still need to be examined and are not included in the scope of this study. Since the secondary circuit is not activated, and the presence of radioactive gases is excluded, it is reasonable to assume that the design of these remaining components will be simpler that in the primary circuit.

The method for extracting the secondary loop form the overall facility is illustrated in the next following figures.

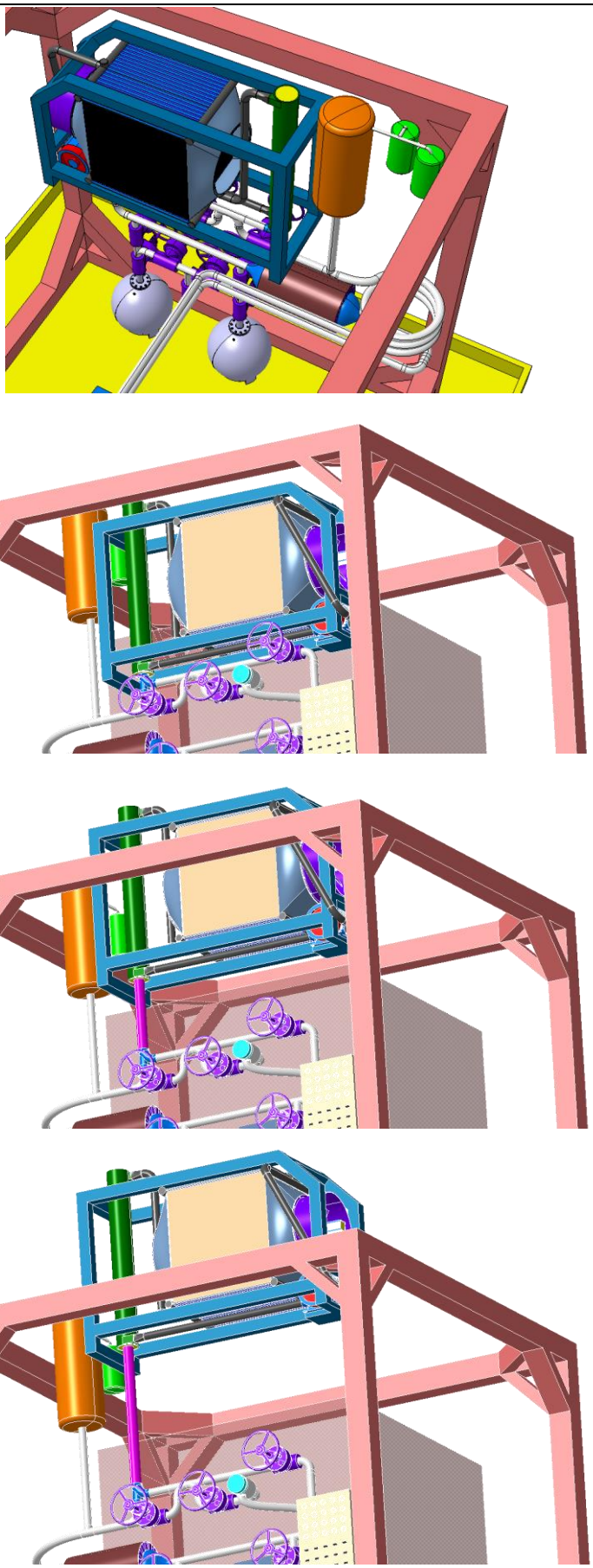

Figure 26: Extraction of the secondary circuit

2.1 Secondary heat exchanger

The secondary heat exchanger cools the secondary fluid down to 75°C after being heated to 120°C by the primary fluid in the primary heat exchanger. The proposed design is a plate heat exchanger cooled by forced convection air at 20°C. In these conditions, approximately 10 m^2 of exchange surface allows 100 kW of heat to be extracted.

The secondary fluid flows from a collector at the bottom of the plate exchanger to the top collector from where it passes back on to the inlet of the primary heat exchanger as indicated by the arrows in the figure below.

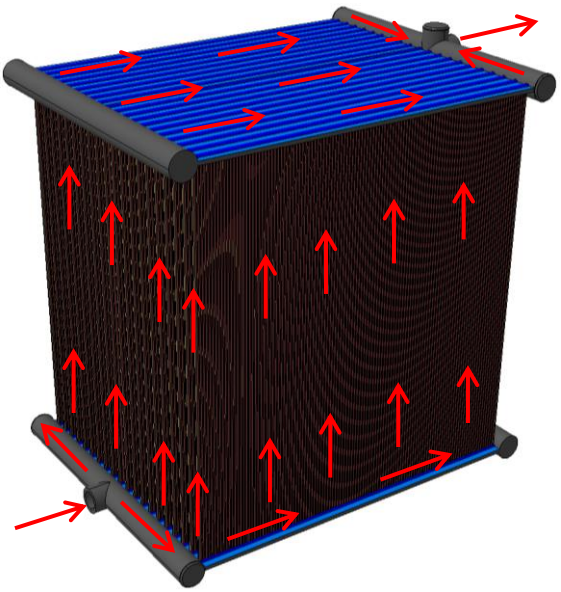

Figure 27: Secondary heat exchanger

The airflow along the plates is channelled by an inlet and outlet cone driven by an electrically motorized propeller.

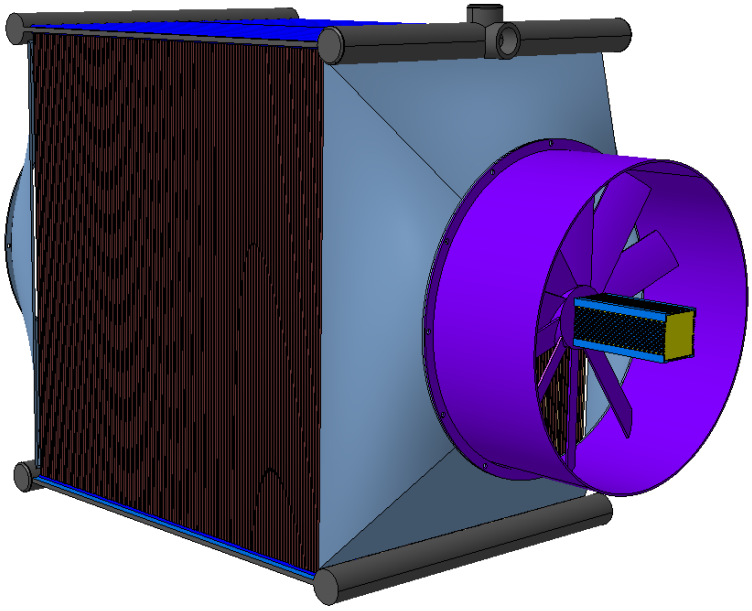

Figure 28: Secondary heat exchanger air cooling

2.2 Permanent magnet electromagnetic induction pump

As in the primary loop, a pump is needed for the secondary loop able to cope with liquid metal. The working principle is slightly different from the electromagnetic pump in the secondary and is driven by rotating permanent magnets as shown in the reference http://ipul.lv/main/?nav=imants

The pump must be able to provide a flow rate of 3,5 m3/h with sufficient power to overcome the drag losses in the fin plates. This matter will be analysed in the second stage of the project.

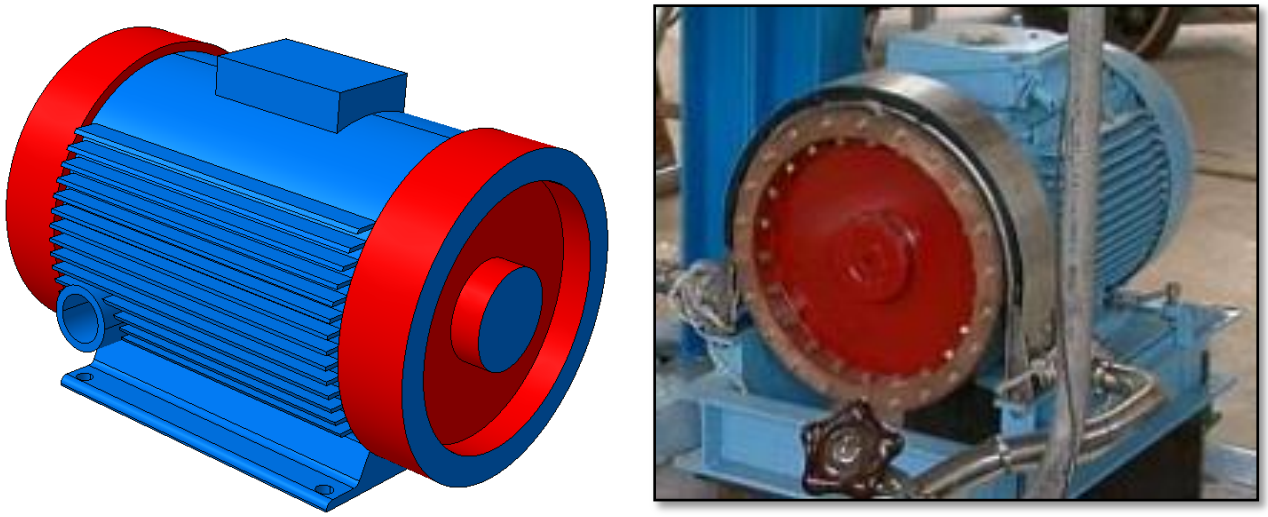

Figure 29: Permanent magnet electromagnetic induction pump

2.3 Pneumatic power

The power for actuating the valves should come in part from a pneumatic accumulator with a corresponding power panel and gas compressor. This will provide some redundancy in terms of not relying only on electric power which is susceptible to damage from radiation. To allow easy access, the power panel is positioned below the valve farm and the compressor should be placed in the lower corner as illustrated in the figure below.

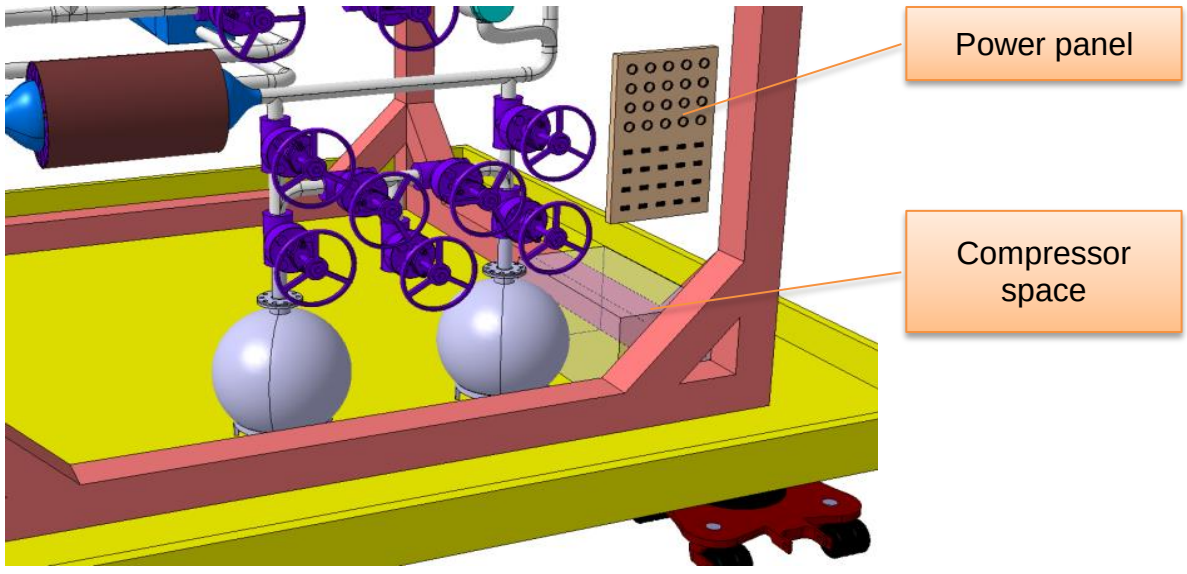

Figure 30: Pneumatic power

3 Effect of transients in the facility

The calculation of transients in the heat exchanger could not fit within the scope of the current engineering concept phase. It is therefore discussed qualitatively.

3.1 Loss of flow

The immediate effect of the loss of the EMP is a coast down until natural circulation conditions are reached. As in a conventional NPP, the cold source in effect the heat exchanger is situated at the top of the loop. The heat source on the other hand is at almost the lowest position in the loop.

A gravity driven flow may therefore be expected due to the effects of buoyancy. Since every effort has been made to keep the drag penalty in the primary circuit small, the progression form driven flow thru coast-down to gravity-driven flow may be expected to be progressive, giving ample time to switch off the beam before the reduced flow on the window may lead to its failure.

A full study of this effect would include using traditional safety codes such as RELAP/CATHARE/NRC-TRACE and extracting the integrated time-dependent flow rates to apply as boundary conditions to a full CFD couple with a thermal-stress analysis of the beam window area.

3.2 Beam transient

Occurrences of the beam switching off and then back on are certain; in which case a “cold slug” followed by a “hot slug” will flow through the primary circuit when the beam switches on again. This can be simulated by starting a calculation in steady state at the low temperature and then increasing suddenly the temperature at the inlet to hot temperature over a period of roughly 1 [ms].

The most sensitive elements in the loop will be the beam window and to a lesser degree the heat exchanger, which will be protected by the inertia of the loop.

The study should also cover thermal stresses. Natural circulation is less severe for stresses and can be neglected. The effects on the gap in the heat exchanger are possible, although stresses are likely to be small due to the compensating effect of the corrugated copper sheet. In any case it is necessary to transfer the temperature maps to a structural model along with the pressure maps and calculate the stresses.

4 Conclusions

A design for the irradiation facility has been proposed and laid out in sufficient detail to demonstrate the feasibility from a technical standpoint. The level of detail is sufficient for a rough cost estimate of the facility to be made at project level (Ref.6). The design reflects the latest progress made in the neutronics which were documented in Ref.4 and in the hydraulic design of the target as per Ref.3. Hence an engineered solution has been found which fulfils all the requirements laid out in the specification, with regards to a facility able to irradiate samples at high doses.

The design features some innovative solutions such as the dismountable heat exchanger in which the secondary and primary loop are physically separate with no common wall. The secondary loop is easily removable form the facility, easing maintenance and the management of possible leaks. Another innovation lies in the target itself which can absorb a specially tailored elliptical profile beam, thus exposing the samples to a high DPA. This is made possible by the design of a window with an elliptical base and is optimised in terms of stress and cooling (Ref.3). The loading mechanism for the samples is equally new. It can load samples cyclically using mechanisms which are easily dismountable from the target, which enhances its capability to accommodate many experiments.

A very robust engineering solution has been found, which addresses the need for testing materials at high irradiation doses, whilst keeping the overall facility compact enough for it to be transportable and adaptable to many diverse laboratories.